



## Evaluating the effects of historical land cover change on summertime weather and climate in New Jersey: Land cover and surface energy budget changes

Paul S. Wichansky,<sup>1</sup> Louis T. Steyaert,<sup>2,3</sup> Robert L. Walko,<sup>3</sup> and Christopher P. Weaver<sup>1</sup>

Received 2 June 2007; revised 26 July 2007; accepted 29 November 2007; published 28 May 2008.

[1] The 19th-century agrarian landscape of New Jersey (NJ) and the surrounding region has been extensively transformed to the present-day land cover by urbanization, reforestation, and localized areas of deforestation. This study used a mesoscale atmospheric numerical model to investigate the sensitivity of the warm season climate of NJ to these land cover changes. Reconstructed 1880s-era and present-day land cover data sets were used as surface boundary conditions for a set of simulations performed with the Regional Atmospheric Modeling System (RAMS). Three-member ensembles with historical and present-day land cover were compared to examine the sensitivity of surface air and dew point temperatures, rainfall, and the individual components of the surface energy budget to these land cover changes. Mean temperatures for the present-day landscape were 0.3–0.6°C warmer than for the historical landscape over a considerable portion of NJ and the surrounding region, with daily maximum temperatures at least 1.0°C warmer over some of the highly urbanized locations. Reforested regions, however, were slightly cooler. Dew point temperatures decreased by 0.3–0.6°C, suggesting drier, less humid near-surface air for the present-day landscape. Surface warming was generally associated with repartitioning of net radiation from latent to sensible heat flux, and conversely for cooling. While urbanization was accompanied by strong surface albedo decreases and increases in net shortwave radiation, reforestation and potential changes in forest composition have generally increased albedos and also enhanced landscape heterogeneity. The increased deciduousness of forests may have further reduced net downward longwave radiation.

**Citation:** Wichansky, P. S., L. T. Steyaert, R. L. Walko, and C. P. Weaver (2008), Evaluating the effects of historical land cover change on summertime weather and climate in New Jersey: Land cover and surface energy budget changes, *J. Geophys. Res.*, *113*, D10107, doi:10.1029/2007JD008514.

### 1. Introduction

[2] Although humans have continually shaped the landscape for centuries, it has only been within the past two decades that land use and land cover change (LULCC) has been recognized as a key proximate driving force of global environmental change [Turner, 2001]. With the clearing of native forests and wetlands, the expansion and shifts of agriculture, and the rise of urbanization, the human use of the land has produced a heterogeneous and fragmented global mosaic of seminatural and man-made surfaces [Ramankutty

and Foley, 1999; Klein Goldewijk, 2001]. The physical modification of the landscape that accompanies land cover change, e.g., shifts in surface roughness, albedo, and leaf area index (LAI), alters the key land surface processes (radiation, energy, and soil moisture budgets) that modulate fluxes of heat and moisture at the surface and exchanges between the surface and lower atmosphere [e.g., Segal and Arritt, 1992], thereby influencing the biogeochemical cycles of water and carbon [Claussen *et al.*, 2001]. These changes may also affect surface air temperatures, atmospheric boundary layer properties, convective rainfall, and soil moisture which can influence surface weather and climate across a range of space and timescales [Pielke, 2001]. These changes can, in turn, exert controls on vegetation conditions and ecosystem structure and function which may lead to feedbacks on fundamental land surface processes and interactions at the atmosphere-terrestrial interface [Pielke *et al.*, 1998; Oleson *et al.*, 2004].

[3] Examples of model-based and observationally based studies of large-scale alterations of biophysical parameters

<sup>1</sup>Center for Environmental Prediction and Department for Environmental Sciences, Rutgers University, New Brunswick, New Jersey, USA.

<sup>2</sup>Center for Earth Resources Observation and Science, U.S. Geological Survey, and Biospheric Sciences Branch, NASA Goddard Space Flight Center, Greenbelt, Maryland, USA.

<sup>3</sup>Department of Civil and Environmental Engineering, Duke University, Durham, North Carolina, USA.

due to LULCC include: warming and rainfall pattern shifts resulting from deforestation in tropical regions [Dickinson and Henderson-Sellers, 1988; Claussen et al., 2001; Chagnon et al., 2004; Chagnon and Bras, 2005]; cooling due to replacement of presettlement vegetation with agriculture and other modern land cover types (e.g., pastureland) [Bonan, 1997; Betts, 2001; Zhao et al., 2001; Bounoua et al., 2002; Matthews et al., 2003; Mahmood et al., 2004]; and cooling associated with midlatitude reforestation (i.e., the change from grassland or mixed agriculture to deciduous forest) [Sellers, 1992; Pitman, 2003; Beltrán, 2005]. Other regional LULCC studies have investigated: soil moisture depletion and warming due to overgrazing in the Sonoran desert [Bryant et al., 1990; Balling, 1988]; changes in local cloudiness and rainfall due to landscape changes in Germany [Mölders, 2000]; reductions in summer rainfall, mesoscale circulation changes, and increased severity of winter freeze events due to historical LULCC in South Florida [Pielke et al., 1999; Marshall et al., 2003, 2004a, 2004b]; and the sensitivity of the lower atmosphere to changes in the fractional vegetation as estimated from the satellite-derived normalized difference vegetation index (NDVI) [Bounoua et al., 2000; Zeng et al., 2000], roughness length [Sud et al., 1988], and LAI [Chase et al., 1996]. Many of these studies emphasize the importance of designing land surface schemes that can effectively parameterize subgrid-scale landscape heterogeneity in global-scale climate models (e.g., as raised by Avissar and Pielke [1989]). In addition to altering biophysical properties, LULCC can also influence weather and climate because of changes in the spatial heterogeneity of the land cover and corresponding impacts on mesoscale circulations that affect surface temperatures, clouds, and rainfall [e.g., Anthes, 1984; Pielke and Avissar, 1990; Pielke et al., 1991; Cutrim et al., 1995; Lynn et al., 1995; Avissar and Liu, 1996; Avissar and Schmidt, 1998; Brown and Arnold, 1998; Baidya Roy and Avissar, 2000; Weaver and Avissar, 2001; Baidya Roy et al., 2003a].

[4] Urbanization is an extreme conversion of land cover within highly populated regions [Taha, 1997; Arnfield, 2003]. Empirical studies have documented how urban growth during the 20th century has led to observed increases in the mean and diurnal minimum temperature in developed areas, and decreases in the diurnal temperature range [Karl et al., 1988, 1993; Gallo et al., 1996; Gedzelman et al., 2003; Kalnay and Cai, 2003]. The removal of vegetative cover and expansion of impervious urban surfaces combine to reduce evaporative cooling and lead to additional warming. Other impacts of urbanization can include enhanced rainfall amounts over and downwind of major cities [Bornstein and Lin, 2000; Shepherd et al., 2002; Shepherd and Burian, 2003]. Numerical studies [Sailor, 1995; Avissar, 1996; Xiao et al., 1998] have shown that urban vegetation can have a moderating influence upon the local metropolitan climate. In coastal regions, the meteorological impact of a city interacts with the sea breeze circulations, contributing to the ventilation of elevated urban temperatures [Yoshikado, 1990, 1992; J. Nielson-Gammon, preprint, 2000]. The interactions of these climate change impacts on the urban atmosphere are highly nonlinear and still not well understood [Rosenzweig and Solecki, 2001; Shepherd, 2005], emphasizing the need for more research, including into improved land surface

parameterizations in urban climate models [Grimmond and Oke, 1999; Niyogi et al., 2006].

[5] Although several mesoscale modeling studies have investigated the potential consequences of LULCC in North America from the natural vegetation prior to European settlement to the present-day seminatural land cover [see Copeland et al., 1996; Pielke et al., 1999; Eastman et al., 2001; Baidya Roy et al., 2003b; Marshall et al., 2004a, 2004b; Schneider et al., 2004], few modeling studies to date have examined the potential effects of land use change within a highly populated, urban region that was once primarily agricultural and forested in the late 19th century. The northeastern United States (U.S.) is among those regions of the world that has witnessed dramatic changes in land use resulting from extensive agricultural, silvicultural, urban, and industrial development during the last century. This paper evaluates the sensitivity of weather and climate to historical changes in land use and land cover for the entire state of New Jersey (NJ) and surrounding regions, a heavily urbanized area that has seen pronounced surface changes. To accomplish this, we take advantage of a newly developed, high-resolution data set of 1880s-era land cover reconstructed from detailed topographical maps. We apply this reconstruction, along with present-day land cover derived from Landsat Thematic Mapper (TM) imagery, in simulations of a summertime drought period using the Regional Atmospheric Modeling System (RAMS).

[6] The primary objectives of this study are (1) to document and describe the direction and magnitude of land cover change over a roughly century-long period (1880s to 1992) for a highly urbanized region that was once predominantly agricultural and forested and (2) to identify and quantify the impact and sensitivity of these land cover changes on surface air and dew point temperatures, rainfall, surface heat and radiative fluxes, and mesoscale interactions during an extreme climatological episode (i.e., a prolonged drought).

[7] This paper is the first in a two-part series that describes some of the regional weather and climate effects potentially associated with documented LULCC. We show how landscape conversions in NJ may have modified surface climate by altering albedo and other components of the land surface energy budget. We also identify, within our region, three land cover change themes (urbanization, reforestation, and deforestation) to demonstrate how each theme could have modified surface climate over the mean diurnal cycle. In a second paper, we examine the effects of land cover change on the thermodynamics and dynamics of the boundary layer, including potential changes to clouds and convection. We also evaluate the effects of increased landscape heterogeneity on the development of inland mesoscale circulations and the associated interactions with the coastal sea breeze front.

[8] Section 2 describes the reconstruction of historical and present-day land cover data sets for NJ and its surrounding states and discusses the RAMS model configuration. Section 3 presents the results, including a comparison of documented land cover changes between the 19th and 20th centuries for this region, and evaluates the sensitivity of regional weather and climate to these

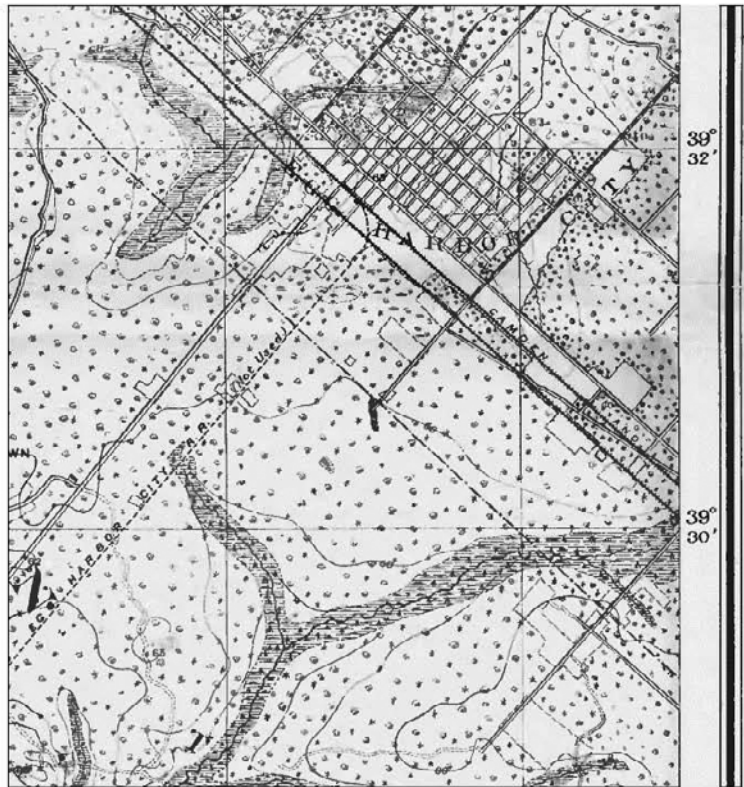


**Figure 1.** A sample portion of the Cook map series, showing the land cover of the Atlantic County area of NJ as it appeared in the late 19th century. The city of Egg Harbor is near the top of the image. Note the mixed forest to the south of Egg Harbor City, while the forested wetlands are represented by finely spaced horizontal lines that imply saturated soil conditions.

historical land cover changes. Section 4 provides a summary and conclusions.

## 2. Methodology and Model Configuration

### 2.1. Historical Land Cover Reconstruction

[9] The 19th-century land cover data set for NJ used in this study was reconstructed from a series of topographical maps that were created under the direction of Dr. George H. Cook, a renowned state geologist and educator. As the first director of the New Jersey Agricultural College Experiment Station in 1880, Dr. Cook, along with his colleagues, created a detailed topographical atlas of the entire state, thereby documenting the distribution of wetlands, forests, and other land cover types that described a relatively rural landscape in the circa 1880 time period [Vermeule, 1889]. New Jersey thus became the first state in the nation to have its official geological survey completed with the mapping of 19th-century land cover information [Sidar, 1976] on a scale of one inch to one statute mile, or 1:63,360 [Letts, 1905]. This topographical atlas was mapped to a rectangular polyconic projection, which was a projection derived and used by the U.S. Coast and Geodetic Survey in the latter half of the 19th century [Schott, 1882]. Figure 1 shows a representative portion of the map series (hereafter referred to as the Cook map series) which was mapped at a sufficiently detailed spatial resolution to conduct our historical land cover change analysis.

[10] We interpreted and manually digitized the information contained in the Cook map series to create a high-resolution, gridded land cover database of the state's vegetation, wetlands, surface water, and built-up areas during the 1880s era. For all 17 maps in the series, we manually estimated and aggregated the fractional percentages of 14 seminatural land cover types depicted on the maps, in increments of 10%, within 2.0-arcminute latitude-longitude grid cells [Wichansky *et al.*, 2006]. This translated the state into a gridded domain of  $51 \times 74$  cells; for the mean latitude of NJ ( $40^\circ\text{N}$ ), the approximate zonal (west-east) and meridional (north-south) cell widths were 3.71 km and 2.84 km, respectively. Estimating the fractional areas of land cover in increments finer than 10% was not feasible. Table 1 lists these 14 land cover types. Appendix A1 describes in more detail the procedures we used to identify these and other historical land cover types on the Cook map series (e.g., urban areas, agricultural land), as well as estimate their corresponding fractional areal percentages within each grid cell.

[11] As will be discussed below in section 2.4, the boundaries of our model simulation domain encompass not only NJ, but also parts of adjacent states or regions that include Pennsylvania (PA), New York (NY)/Long Island (LI), Delaware (DE), and Connecticut (CT). We created a historical land cover data set for this broader region using county-level data from the 1880 U.S. Census, which represents the best existing regional land cover

**Table 1.** The 1880s-Era Land Cover Types Identified on the Cook Map Series

Forest Type	Nonforested Wetlands	Forested Wetlands	Other Surface Types
deciduous forest, pine forest, mixed forest	cranberry bogs, freshwater marsh, tidewater marsh, moist swamp, peat	pine swamp, cedar swamp	pasture land, short grass, beach, water

information available to reconstruct the historical landscape for these states adjacent to NJ. The county-level census data include observed estimates on the total acreage of improved and unimproved farmland in each county where improved farmland was further delineated as either tilled land or meadow-pastureland, while unimproved farmland corresponds to forests and woodlots [*U.S. Bureau of the Census*, 1960; *Waisanen and Bliss*, 2002]. The fractional areal percentages derived from these acreage estimates for the surrounding states were then binned into four broad land cover categories: mixed agriculture, deciduous forest, pastureland, and an “other” category for nonfarmland types such as towns or, in some cases, seminatural vegetation types. Appendix A2 describes the data adjustments that were required to ensure that our census-based reconstruction was reasonably consistent with known historical land use.

[12] Once we gridded these county-wide averages of interpreted land cover to the same 2.0-arcminute mesh as that of the Cook map series, and then merged it with the NJ land cover data, we were able to reconstruct a continuous 1880s-era land cover data set for the entire region.

## 2.2. Present-Day Land Cover

[13] Our present-day land cover data set was adapted from the U.S. Geological Survey (USGS) 1992 National Land Cover Data set (NLCD) [*Vogelmann et al.*, 2001]. On the basis of Landsat TM data from 1992 and 1993, this 30-m resolution data set was designed for use in environmental, land management, and regional modeling applications. Its land cover classification consists of 21 hierarchical classes in a modified Anderson Level II scheme [*Anderson et al.*, 1976]. For this study, we first aggregated the 30-m NLCD to a 1-km grid according to the dominant land cover class, and further aggregated the resulting data to a 2.0-arcminute grid. This aggregation technique is similar to that described by *Steyaert and Pielke* [2002].

[14] Because the land cover categories defined by the Cook map series (and in the 1880 census data) differ from those of the NLCD Anderson II classification, we reconciled the historical and present-day data sets and remapped each to a common, simplified set of eight land cover classes. These simplified classes are (1) combined agricultural and pastureland, (2) deciduous broadleaf forest, (3) mixed deciduous and evergreen forest, (4) evergreen needleleaf forest, (5) marshes and other treeless wetlands, (6) forested wetlands, (7) urban areas, and (8) surface water. Each of these eight categories represent (with minor modifications) a standard land cover type (or mixture of two types) in the RAMS land-surface scheme, described in section 2.3. We carried out this reconciliation and remapping to avoid introducing any spurious land cover changes into our

surface data sets, preventing us from potentially classifying the same land cover into two different categories. This strategy helped us isolate, within our region, the actual land use changes from the late 19th century to the late 20th century.

[15] Because water can be an important land cover class at the regional scale, we made assumptions about the relative distributions of lakes and other inland surface water bodies between the various data sets. The census does not have a land cover category to represent inland water, so we overlaid all lakes, rivers, and inland water that were present in the NLCD (using the final 2.0-arcminute grid resolution) onto the census data for those states that surrounded NJ. This adjustment made the 1880 census and NLCD inland water distributions virtually identical, ensuring that inland water bodies did not abruptly shift their locations between these two time slices of the same region. Therefore, outside NJ, there is no change in the distribution of inland surface water from the 1880s to the 1990s in our reconstruction. Within historical NJ, however, we used the inland water data from the Cook map series.

[16] One of the key characteristics of the Cook map series data is the rough correspondence on the level of detail between the 1880s-era topographical maps and the aggregated 1-km present-day land cover that was derived from satellite data analysis. The relatively fine spatial details of these data sets for NJ make interpretation of probable shifts in land cover features much easier. For those areas outside NJ, however, some of the differences between our historical and present-day reconstructions (e.g., in the degree of fragmentation of the landscape) are likely artifacts due to differences in effective resolution between the 1-km NLCD data and the county-level census data. The interpretation of observed land cover changes within the broader region should also consider these differences in mapping scales.

## 2.3. RAMS Model Description

[17] The simulations presented in this study were performed using the three-dimensional atmospheric RAMS model, version 4.3, in its nonhydrostatic mode [*Walko and Tremback*, 2000; *Cotton et al.*, 2003]. Our model included parameterizations for subgrid-scale transport [*Mellor and Yamada*, 1982], convection [*Kain and Fritsch*, 1992], microphysics [*Walko et al.*, 1995], and radiative transfer [*Harrington*, 1997]. RAMS was coupled to the Land Ecosystem-Atmosphere Feedback Model, version two (LEAF-2) [*Walko et al.*, 2000], a module that estimates vertical energy and water exchange between the soil, vegetation, and overlying atmosphere for multiple patches of land cover within a single grid cell. LEAF-2 assimilates land cover data sets to define the surface-atmosphere boundary. Land surface parameters (LSPs), including surface albedo, leaf area index, fractional vegetative cover, roughness length, and displacement height, can be prescribed according to land cover type and time of year. The values assigned to these LSPs generally correspond to those of the standard Biosphere-Atmosphere Transfer Scheme (BATS) vegetation categories [*Dickinson et al.*, 1993].

[18] To simulate the effects of 19th- versus 20th-century land cover in RAMS, we initialized LEAF-2 with our historical and present-day data sets, as mapped to the eight

**Table 2.** Historical and Present-Day Land Cover Classes and Their Reclassification to a LEAF-2 Category in RAMS<sup>a</sup>

Historical Land Cover Classes	NLCD Present-Day Land Cover Classes	LEAF-2 Land Cover Class
Agriculture, pastureland, beach	mixed crop, pastureland, shrubs, grassland, bare rock, sand, other grains	agricultural and pastureland
Deciduous forest Mixed forest	deciduous broadleaf forest, orchards mixed forest	deciduous broadleaf forest mixed forest with LEAF-2 displacement heights reduced by 5.0 m
Evergreen forest Cranberry bogs, tide and freshwater marshes, peat, moist swamps	evergreen needleleaf forest nonforested wetlands	evergreen needleleaf forest nonforested wetlands, initialized with fully saturated soil below a 10-cm depth, with 85% and 88% saturation for the two topsoil layers above 10 cm
Pine swamp, cedar swamp	forested wetlands	50% deciduous shrub and 50% modified mixed forest, initialized with fully saturated soil below a 10-cm depth, with 85% and 88% saturation for the two topsoil layers above 10 cm
Urban	residential/commercial/industrial area	urban
Water	water	water

<sup>a</sup>The historical and present-day land cover classes, as noted in the first two columns, were reclassified to one of the eight LEAF-2 classes that represented a common set of land cover categories applied to both data sets.

categories described above in section 2.2. Table 2 provides a cross reference that matches each of the Cook-Census reconstructed and NLCD classes with the corresponding LEAF-2 categories. Because the coverage of some NLCD classes, including bare rock and sand, were not explicitly mapped during the late 19th century, we reclassified them in our model as agricultural and pastureland.

[19] We made two modifications to the standard LSPs in LEAF-2 to more realistically reflect the surface characteristics of seminatural land cover types in the region. These changes include modifying the displacement height of trees in our mixed forest class, and also specifying the vegetation and soil moisture properties that characterize the forested and nonforested wetlands that are prevalent in NJ. Refer to Appendix B for a more detailed description of these modifications.

#### 2.4. RAMS Model Configuration

[20] The simulation domain was centered over NJ at 40.1°N and 74.6°W. We configured RAMS with three nested grids (Figure 2): grid 1, 1600 km × 1800 km with 32-km horizontal grid spacing, covering much of eastern North America and adjacent ocean (50 × 56 points); an intermediate grid 2, 560 km × 624 km with 8-km spacing (70 × 78 points); and grid 3, 284 km × 284 km with 2-km spacing, covering NJ and portions of its surrounding states (142 × 142 points). This nested grid configuration allows us to downscale the time-varying large-scale (synoptic) forcing into appropriate lateral boundary conditions for the fine-grid domain, on which we can more faithfully capture the details of the small-scale atmospheric dynamics (e.g., sea breezes and inland mesoscale circulations) that respond most closely to the surface forcing. We used a 60-s time step on grid 1 with progressively shorter time step intervals on the two inner grids. Each grid used the same, stretched vertical coordinate (38 levels), ranging from  $\Delta z = 50$  m at the surface to  $\Delta z = 1500$  m at and above 14 km to the model top at 22 km. We also defined 11 soil layers down to a depth of 2.5 m, with soil layer thicknesses, descending from the surface, of 5, 5, 10, 10, 10, 20, 20, 20, 50, 50, and 50 cm. Convection was parameterized using the *Kain and Fritsch*

[1992] scheme on the two outermost grids, but not on the innermost. Thus, convective-scale dynamic processes were modeled explicitly, to the extent possible, on the finest grid (grid 3). While schemes such as Kain-Fritsch have been designed to operate at coarser grid scales than the 8 km of grid 2, the model dynamics alone cannot resolve convection at this grid scale, and so employing a cumulus scheme on grid 2 is the best choice currently available. Note that there is no double counting of precipitation in RAMS when both cumulus parameterization and bulk microphysics are operating, so this is not an issue when using the Kain-Fritsch scheme on grid 2.

[21] We carried out two sets of RAMS simulations: one with 1880s-era land cover for NJ and its immediate

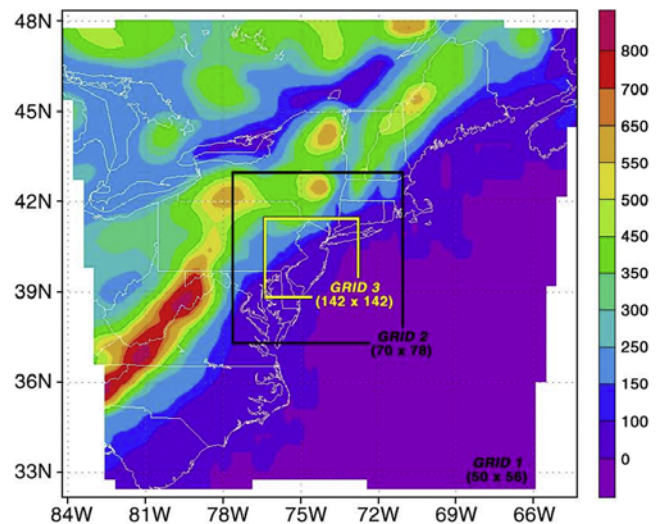


**Figure 2.** Geographical configuration of the parent grid (grid 1), and the two embedded grids, used in the RAMS ensemble runs with simulated historical and present-day land cover. The contours represent the elevation of the model surface, in m, above mean sea level. The numbers in parentheses indicate the number of horizontal grid cells within the respective domain.

surroundings and one with present-day land cover. To isolate the atmospheric response to land cover changes in the region, both sets of model simulations were initialized using identical large-scale atmospheric boundary conditions (described below) with the only difference being the land cover as specified in LEAF-2. We assigned the historical and present-day land cover to grid 3 only, so this grid also represented the full spatial extent of our 1880 census data. For all runs, the NLCD-based land cover was used on grids 1 and 2. In this way, we attempt to isolate the sensitivity of our simulations to land cover changes within and adjacent to NJ. Ideally, we would have preferred to use the census data as the surface boundary on grid 2 in the historical simulations, but given the coarse 40 km effective spatial resolution and limited thematic detail of the reconstructed census land cover, our primary consideration was to take maximum advantage of the unique high-resolution 2-km 1880 land cover data for NJ.

[22] On all grids, we allowed a maximum of six surface types per grid cell (including water) to represent subgrid-scale land cover detail in LEAF-2. The use of this 2-km grid cell size (and its subgrid-scale patches) for our finest grid distinguishes this study relative to other LULCC studies that employ coarser-resolution models. In addition, we also specified a soil type of silt clay loam everywhere.

[23] Initial atmospheric conditions for both sets of simulations were specified using 6-hourly,  $2.5^\circ$  longitude  $\times$   $2.5^\circ$  latitude National Center for Environmental Prediction (NCEP)/National Center for Atmospheric Research (NCAR) reanalysis data [Kalnay *et al.*, 1996]. The first reanalysis data time was used for initializing the entire domain, and subsequent data times were then used for specifying the lateral boundary conditions for the parent grid (grid 1). For each simulation, RAMS was run for 2 months, June–July 1999. This time period coincided with an intense regional drought in the northeastern U.S., with record or near-record high temperatures and heat wave impacts at many locations during July. New Jersey experienced the second driest 4-month period (April to July 1999) in the state’s 105-year historical record [Morehart *et al.*, 1999]. Rainfall deficits were severe enough that, by mid-August, the U.S. Department of Agriculture declared nine states, including NJ, NY, and PA, as agricultural drought disaster areas [Heim, 1999]. The choice of this time period allows us to examine the sensitivity of the regional climate system to land surface properties under extreme conditions and to explore ways in which changes to the landscape over a period of time might affect the severity of prolonged seasonal droughts. In a broader context, the use of 1999 NCEP reanalysis data over historical land cover allows RAMS to simulate what the climate of the summer of 1999 would have looked like if the land surface resembled that of the 1880s rather than the present-day.

## 2.5. Land Surface Initialization and Experimental Design

[24] Since we did not alter the LSPs of our land cover data sets to reflect the persistent drought conditions of June–July 1999, we initialized the land surface state of our model, and its soil moisture, using a spin-up. The month of June was used as our spin-up period and the month of July as our analysis period. We accomplished this spin-up

by running RAMS for one full month (1200 UTC 1 June to 1200 UTC 1 July) using grids 1 and 2 only, forcing RAMS more strongly with the reanalysis boundary conditions (i.e., by using stronger nudging) to ensure that the soil spin-up would be as consistent as possible with the actual atmospheric conditions leading up to the start of our analysis period. For soil moisture at the start of the spin-up period, 1 June, we used a horizontally homogeneous but vertically varying profile on both grids, with 50% saturation at the surface to 70% in the deepest soil layer. This profile is loosely based upon observed soil moisture estimates for NJ and the immediate region during the first week of June 1999 [U.S. Department of Agriculture, 1999]. We disaggregated the 1200 UTC 1 July soil temperature and soil moisture values resulting from the spin-up at each horizontal cell and vertical layer from grid 2, horizontally smoothed these disaggregated fields, and applied them as initial conditions to grid 3 for all sets of simulations (historical and present-day).

[25] Our spin-up strategy is very similar to the approach used successfully by Weaver [2004a, 2004b]. This approach allows for the development of more realistic, heterogeneous, fine-scale soil moisture and soil temperature features by the start of the analysis period that are consistent with the land and atmospheric components of the particular model used (in our case, RAMS). The spin-up was designed carefully to ensure a good match of the July simulations with observations, particularly critical since July 1999 was an anomalous drought period. Therefore, we performed a number of test runs where we varied the soil moisture at the start of the spin-up from these initial 50/70% values and compared modeled and observed trends in near-surface air temperature and dew point into the first few days in July, eventually settling on these values as providing the best overall agreement. We also tested the impact of a longer spin-up on our results and found little systematic difference between a 1-month and 2-month (May–June) spin-up period.

[26] A key feature of our experimental design is the use of ensembles of simulations for both the historical and present-day land covers. This was designed to allow us to average over the effects of internal atmospheric variability and increase the robustness of our findings. Because the simulations were so computationally expensive, we were limited to only three members for each ensemble. We performed a set of three simulations using our reconstructed 1880s-era land cover data and a separate set of three simulations using the NLCD-derived land cover data for the same region. The three simulations for a given land cover data set were each initialized using slightly different model atmospheres that reflected 29 June, 1 July, and 3 July initial conditions. Each simulation is thus started at a different initial time with all three of the simulations overlapping. Specifically, after each spin-up ended (i.e., at 1200 UTC on 29 June, 1 July, and 3 July, respectively), we added the third grid with its specified land cover data set, initialized the land surface state on grid 3 according to the above spin-up procedure, and restarted the simulation, running the model until 0400 UTC 1 August. To obtain ensemble means, we averaged the three simulations over the same model times on grid 3. Arritt *et al.* [2004] discuss this lagged average ensemble method (with lags between ensemble members on the order of a day or so) as an accepted technique for generating

ensembles over monthly to seasonal timescales in nested regional climate simulations. As described above, all six model runs used the same spun-up 1 July soil moisture and soil temperature, allowing us to isolate the atmospheric response to its land cover specification.

[27] Since the analysis period of the 29 June ensemble member was 96 h longer than that of the 3 July ensemble member, because of a shorter spin-up, we distributed the ensemble member weights equally by examining only the period where all three simulations for each ensemble fully overlap in time, from 1200 UTC 3 July to 0400 UTC 1 August. Throughout the rest of the paper, we present our results as the monthly mean difference, on grid 3, between the present-day and historical ensembles at each grid cell (or a composite of grid cells) during this time period.

### 3. Results

#### 3.1. Documented Land Cover Changes

[28] Significant differences between the 1880s-era and present-day landscapes are apparent from the reconstruction data sets, and these differences agree reasonably well with our understanding of the historical transformation of land cover that has occurred within and around NJ during the last century. This includes an extensive regional expansion of impervious surfaces resulting from dramatic urban and suburban growth, a progressive and accompanying loss of agricultural land, both decreases and increases in forest cover (depending on location), and isolated changes in the coverage and extent of wetlands. The result today is a significantly more heterogeneous and fragmented landscape. We summarize these changes in Figure 3.

[29] In the 1880s, central and northern NJ, along with adjacent eastern PA and southern NY, was an area of extensive agricultural land. In the lowlands of eastern PA, for example, mixed agriculture was by far the dominant land cover type during this period [*U.S. Bureau of the Census*, 1960]. Over the ensuing century, however, much of the agricultural land in these regions was lost (Figure 3a), either abandoned and reverted to forest, or developed to create the modern urban and exurban sprawl. Given the intensity of mixed agriculture that once characterized areas like southeastern PA, and the minimal forest cover as described in the 1880 U.S. Census, we believe that the relative lack of spatial heterogeneity of the late 19th-century agrarian landscape in this region is likely real and that it also contrasts realistically with the significantly enhanced heterogeneity evident in our present-day land cover data set, due to these land use processes.

[30] Agriculture was the predominant land cover type in 19th-century NJ. Of all states, NJ was, at that time, first in farm income per acre; the state's economy was historically based upon agricultural exports such as peaches and tomatoes, but began to witness an early 20th-century shift to professionally managed industrial and commercial enterprises [*Cunningham*, 1981]. The geographic location of NJ between the major markets of New York City and Philadelphia helped to foster urban and suburban growth at the expense of agricultural land resources. As a result, the total acreage of NJ farmland sharply declined from 2.9 million acres in 1880 to 848,000 acres by 1992, a decrease of about 70% [*Schmidt*, 1973; *U.S. Department*

*of Agriculture*, 1992]. The higher land values in close proximity to these major metropolitan areas also meant that agricultural production per unit land area could not effectively compete against the profitability of potential suburban land uses such as residential developments or industrial complexes [*Stansfield*, 1998]. Other factors have also been involved. For example, mechanization and advances in plant science have dramatically increased the efficiency of the remaining farms, providing a significant economic advantage to farmers [*Hart*, 1991]. Intensive farming practices that raised agricultural productivity have, unfortunately, also accelerated soil erosion and general land degradation [see *Boardman and Favis-Mortlock*, 2001]. All these factors, including the higher taxes placed upon farmland, technological advances, and shifting socioeconomic drivers, have continued to play a role in transforming NJ's 19th-century agrarian landscape [*Agthe*, 1964].

[31] Apart from this general decrease, some increases in agricultural land use have occurred, notably within the inner coastal plain of southern NJ. Over time, truck farming became a significant boon for the state, as the growing 20th-century transportation network opened up large industrial and consumer markets for NJ farmers. The increasing demand for locally grown produce such as blueberries and spinach made it necessary to form cooperative produce auctions [*Fabian and Burns*, 1966] where fruits and vegetables could be priced competitively and exported to urban markets via railroad and trucks.

[32] The land cover change since the 1880s-era in NJ and the surrounding region is also characterized by patterns of reforestation and deforestation (Figure 3b). Extensive forest regrowth occurred in the northern highlands of NJ and eastern PA following farmland abandonment. In contrast, forest regrowth and deforestation patterns are more localized and heterogeneous in the lowland areas of NJ (see Figure 3b). In addition to farmland abandonment, the present-day forest regrowth also regenerated on burned over lands that resulted from extensive wildfires during the early 1900s prior to fire suppression programs [*Little*, 1979]. Deciduous broadleaf trees are dominant in the present-day NJ forest in terms of total area [*Vogelmann et al.*, 2001] and total tree volume [*Widmann*, 2002]. Comparison of our reconstructed forest cover data for 1880 and the present-day forest cover based on the NLCD classification further suggests increased deciduousness of the forest. For example, red maple has become a common tree in NJ [*Alderman et al.*, 2005]. In addition, landscape fragmentation has probably contributed to increased deciduousness within the present-day land cover due to grasses, shrub, and small deciduous broadleaf tree regeneration following disturbance. The patterns of deforestation, however, are typically associated with residential and urban development such as in northeastern and central NJ (e.g., Ocean County) and near the Atlantic City metro area in the southeastern part of the state (e.g., Atlantic County).

[33] The rapid expansion of urbanization since the late 19th century is strikingly illustrated in Figure 3c. This growth has centered around, and extended outward from, the densely populated cities of Philadelphia and New York, consuming both agricultural and forested lands, as discussed above. Expansive metropolitan areas of residential and commercial suburbs now almost completely cover

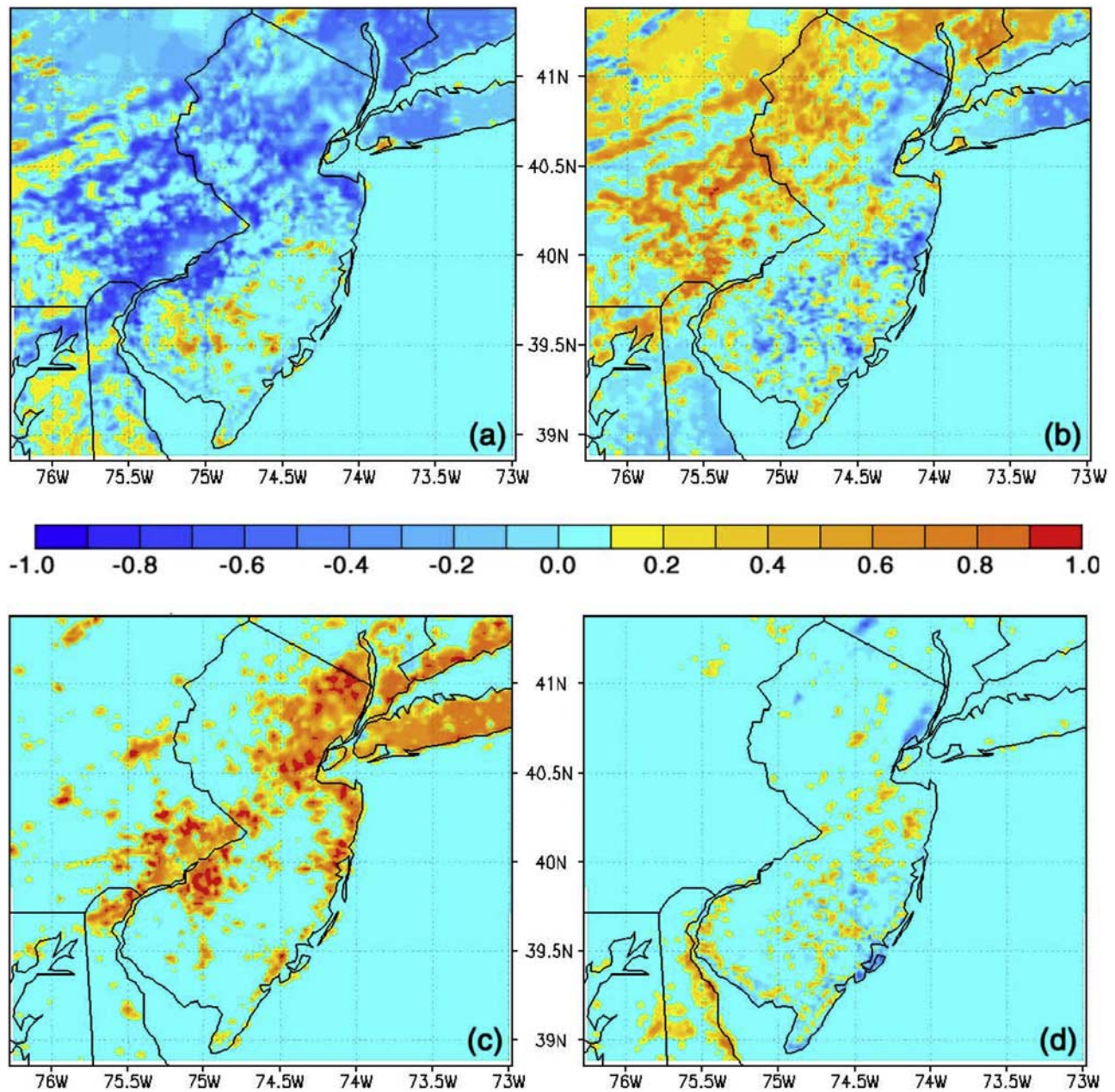


**Figure 3.** Differences in fractional land cover (present-day fraction of total area minus historical fraction of total area), for grid 3, in (a) agricultural and pastureland, (b) total forested area, (c) urban regions, and (d) nonforested and forested wetlands. The contour interval represents the fractional changes in the respective land cover type.

several counties in NJ [Lathrop and Hasse, 2006] and its bordering states. Figure 3c also implies an extensive regional expansion of dry impervious surfaces.

[34] Finally, Figure 3d shows the patterns of wetlands change on the basis of differences between the reconstructed 1880 and the present-day land cover data sets. Because there is much uncertainty in these patterns due to the difficulties in the characterization and inventory of wetlands under any circumstances, these results are supplemented by historical studies. For example, the tidal and freshwater wetlands that originally covered parts of northeastern NJ have been radically altered by various land reclamation

projects, with approximately 108 km<sup>2</sup> of wetlands, as calculated by Vermeule [1897] in an 1896 USGS survey, reduced to 33 km<sup>2</sup> by the late 20th century [Marshall, 2004]. Many of these conversions of wetlands to drylands suitable for agricultural, commercial, and industrial uses occurred prior to shifts in public attitudes toward environmental conservation in the 1960s and 1970s, and the subsequent state and federal legislation. For example, within southern coastal NJ, the wetlands patterns for the 19th and 20th centuries are quite similar, primarily as a result of legislation such as the New Jersey Coastal Wetlands Act of 1970. However, the implied wetland increases in DE are an

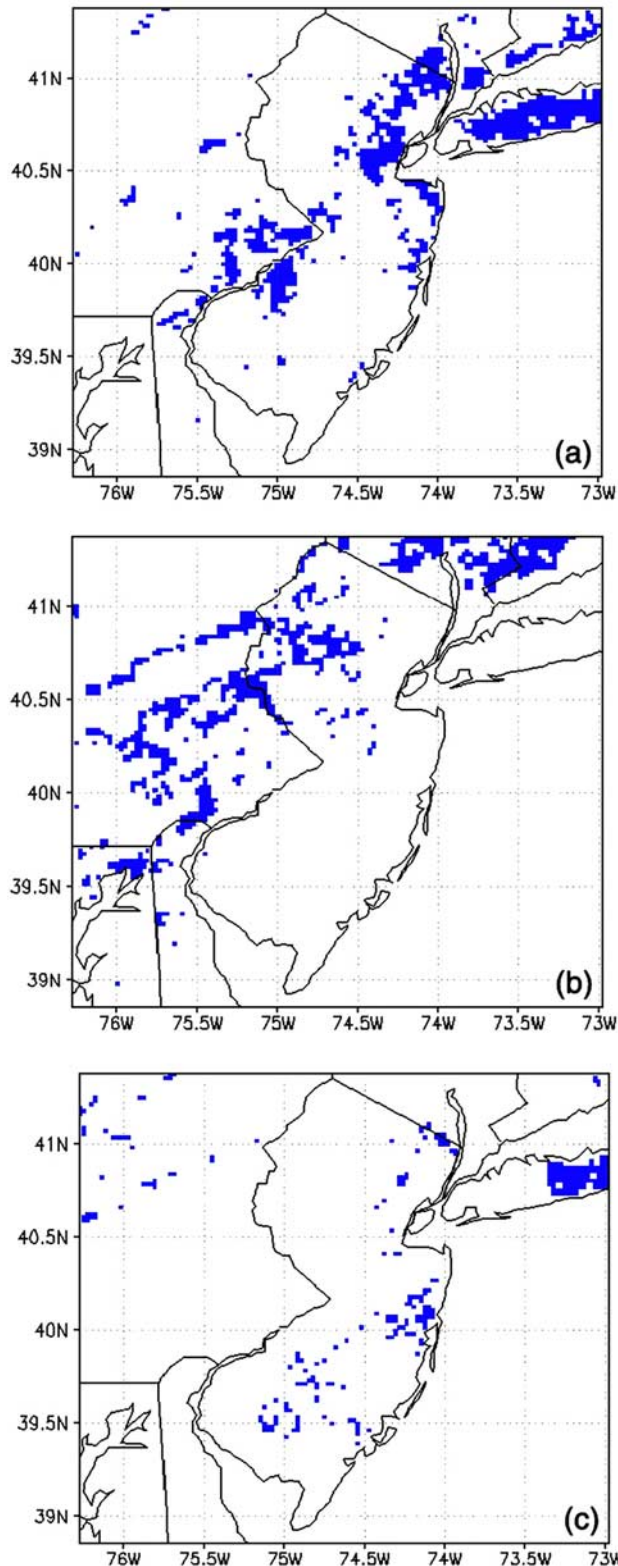


**Figure 4.** The respective grid cells, shown shaded in blue, which have experienced a change in dominant land cover between the historical and present-day data sets. For these grid cells, the dominant land cover changes have resulted from (a) urbanization, (b) reforestation, and (c) deforestation. See text for a more precise description of these definitions.

artifact because the 1880 census data did not include a wetlands category. In addition to difficulties and accuracy issues associated with the mapping of small, highly localized wetland areas, the differences in grid resolution and map projections between the Cook map series and NLCD, combined with the manual digitization procedure we used to reconstruct the historical land cover for the state, probably introduced some biases into the observed changes compared to those for the other land cover types. Together, these can yield additional spatial uncertainties in our documented wetlands change within NJ.

[35] The land cover changes shown in Figures 3a–3d are accompanied by a remarkable transition from a relatively homogeneous 19th-century land surface to one that has become heterogeneous and fragmented. Specifically, the present-day landscape of N.J. is characterized by a heterogeneous mosaic of deciduous, mixed, and evergreen forests interspersed among fields, farms, wetlands, towns, adjacent suburbs, and large urban areas. In coastal and south-central NJ, for example, there is probably an increased deciduousness in the land cover due to changes in forest composition, regenerating vegetation associated with disturbance, isolated patches of increased agricultural and pastureland, and forested wetlands change. The combination of these seminatural vegetation patterns have increasingly fragmented the late 19th-century land surface, and together with some urban development and encroachment onto formerly agricultural or forested land, have significantly enhanced its spatial heterogeneity. These changes can have important effects on the land surface energy budget.

[36] Figure 4 summarizes the principal trends illustrated in Figure 3 with three main themes that reflect the 19th to 20th century shift in NJ and environs from a region dominated by agriculture to a heterogeneous mosaic of cities and suburbs, forests, fields, and farms: urbanization (Figure 4a), reforestation (Figure 4b), and localized deforestation patches (Figure 4c). Here we show only those grid cells where the dominant land cover shifted from one type to another between the historical and present-day reconstructions. For example, Figure 4a shows those cells for which forest and agriculture had at least 50% fractional coverage in the historical reconstruction but more than 50% urban fractional coverage in the present-day reconstruction. Similarly, Figure 4b shows those grid cells that converted from dominant agriculture to dominant forest, and Figure 4c shows a localized conversion from forest to any nonforest land cover type. We return to these three themes later in the paper as a way to highlight general ideas about the impact of different land conversions on interactions between the land surface and the atmosphere, specifically by compositing various climatological variables over these different sets of grid cells. According to these themes, 17% of all land surfaces in the region have been affected by urbanization, 22% by reforestation, and 8% by deforestation. Note that we have used a threshold of 50% (applied to both the historical and present-day data sets) to identify grid cells with one of these conversions, which we consider to be somewhat arbitrary, as different criteria would include or exclude different percentages. Applying

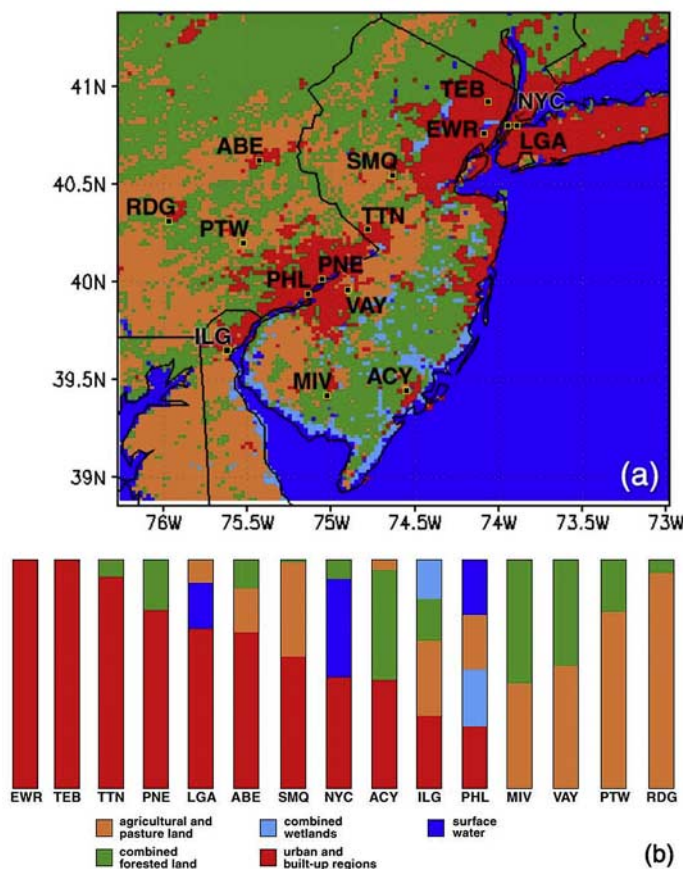


**Figure 5.** (a) The distribution of present-day land cover types for NJ and its surrounding states, derived from the NLCD data set, and (b) the relative areal percentages of these land cover types for the fifteen stations identified where hourly temperature and rainfall observations were available for July 1999. The colors represent the dominant land cover type at the nearest grid 3 cell: forested (green), agricultural and pastureland (orange), wetlands (light blue), urban (red), and water (dark blue).

different threshold values, however, would not qualitatively affect our conclusions.

**3.2. Model Evaluation**

[37] We evaluated our model by comparing temperatures and dew points, as simulated in the present-day ensemble of RAMS runs (hereafter referred to as the control run ensemble), with observations from 15 surface weather stations within the region. These stations, as shown in Figure 5a, are located within grid cells that have a variety of present-day land cover types (Figure 5b). Some of these locations have a large fraction of urban cover, while other locations are characterized by patches of forested land, surface water, or other vegetation types with varying fractional coverage.

[38] Mean observed and model-simulated air and dew point temperatures for July 1999, listed in Table 3 for each station, indicate that observed temperatures (both air and dew points) are generally warmer than those of the control run ensemble. Over all 15 stations, observed surface air and dew point temperatures averaged 1.5°C and 1.8°C higher, respectively, than those of the control run ensemble, implying that our model underestimates air and dew point temperatures.

[39] At least for temperature, the majority of this cool model bias comes from the grid cells containing three stations

located closest to the coastline (ACY, NYC, and LGA). The model temperatures at these stations averaged 4.8°C cooler than observed values. It is likely that systematic errors arising from the use of monthly mean sea surface temperatures, and/or the fact that these grid cells in RAMS contained fractional amounts of ocean as well as land, contributed to these larger biases. We have thus removed these coastal stations from the regionally averaged time series, described below.

[40] The time series of observed and model-simulated air temperatures and dew points, averaged over the remaining twelve “inland” stations and shown in Figure 6, suggests that the control run ensemble captures reasonably well the overall day-to-day trends throughout July. The model was generally able to reach daily maximum and minimum temperatures during the full simulation period (Figure 6a), with periods of more pronounced cool bias in minimum temperatures during the second half of the month (also visible in the dew points, Figure 6b). The time series of the mean standard deviations of these variables (over all twelve stations) for the control run ensemble, also shown in Figure 6, are rather small, suggesting that the different model atmospheres are reasonably consistent for temperature and dew point during the month. Varying the soil type and the initial soil moisture and temperature (at the start of

**Table 3.** Mean Monthly Comparison of Temperatures and Dew Points Between Model and Observations<sup>a</sup>

Station	July Mean Temperatures		RMSE Temperatures	July Mean Dew Points		RMSE Dew Points
	Observed	Simulated		Observed	Simulated	
EWR	27.1	24.4	3.69	17.6	16.0	2.92
TEB	27.1	24.4	3.56	17.3	16.0	3.01
TTN	26.8	26.3	2.83	16.9	16.0	2.66
PNE	27.4	26.5	2.93	19.1	15.7	4.06
LGA	27.5	22.7	5.15	17.5	16.0	2.87
ABE	26.0	27.5	3.00	15.9	15.9	2.48
SMQ	25.9	26.5	3.39	17.4	16.1	2.64
NYC	27.3	22.9	4.77	17.4	16.1	2.62
ACY	26.0	20.9	5.60	18.5	16.1	3.48
ILG	26.8	25.4	3.81	19.1	16.3	3.53
PHL	27.6	26.3	3.15	19.0	16.0	3.81
MIV	25.6	23.0	4.07	19.1	16.2	3.61
VAY	26.7	25.6	3.25	18.6	16.0	3.62
PTW	26.4	27.4	3.19	16.4	16.0	2.54
RDG	26.5	27.6	2.93	16.9	16.0	2.51
Regional average	26.7	25.2	3.69	17.8	16.0	3.09

<sup>a</sup>This is a comparison of the mean monthly observed air and dew point temperatures with the corresponding model-simulated values along with the respective RMSE for July 1999. The simulated air and dew point temperatures represent a mean layer average of the lowest 50 m of the model atmosphere. All units are in degrees Celsius.

our spin-up period) did not qualitatively improve these comparisons between model and observations.

[41] Finally, the observed and model-simulated July rainfall totals, averaged over the twelve stations, were 13.2 mm and 13.1 mm, respectively. These are very light monthly amounts that underscore the severity of the regional drought and indicate that, in the broadest terms, it was adequately captured by our model.

### 3.3. Simulated Differences in Temperatures and Rainfall With Historical Versus Present-Day Landscapes

[42] Within NJ and its adjacent states, we have described a significant increase in 20th-century urban land cover (with a concomitant loss of 19th-century vegetation) that is reflected in dramatic changes to the landscape's LSPs, including surface albedo, net roughness, and fractional vegetative cover. Vegetated land surfaces have in many areas been largely replaced by impervious surfaces with very different physical properties. Combined with the trends of reforestation and isolated deforestation that have also occurred in the region, these land cover changes have created a modified set of surface boundary conditions for the lower atmosphere, altering the radiative, energy, and soil moisture budgets that help modulate land-atmosphere exchanges and thus influencing weather and climate [Giorgi and Avissar, 1997; Pielke, 2001]. Here we document the simulated change in surface air and dew point temperatures, rainfall, and surface heat and radiative fluxes that have resulted from these land cover changes.

#### 3.3.1. Near-Surface Air Temperatures

[43] Monthly differences in RAMS air temperatures at the lowest atmospheric level of our model (for the present-day ensemble minus the historical ensemble, for each grid cell, hereafter applied to all variables) are shown in Figure 7. Simulated mean temperatures are 0.3–0.6°C warmer for the present-day landscape over a large portion of the NJ coastal plain, with additional increases in northeastern NJ, LI, and southern CT. Most of this warming is generally consistent with the expansion of urban surfaces in the New York City, LI, northern NJ, and Philadelphia metro areas since the late

19th century (e.g., see Figure 4a). The warming that is also evident over the inland coastal plain of southern NJ may be due to some combination of deforestation (Figure 4c) and urbanization, in addition to some potential changes in forest composition. For example, the shallower rooting depths that accompany a simulated increase in total pine forested area in the Pine Barrens of central NJ effectively limits access to deeper soil moisture; the enhanced stomatal resistance contributes to these surface air temperature increases.

[44] In addition, there is a cooling of 0.1–0.2°C for the present-day landscape within eastern PA and northwestern NJ. This cooling has generally occurred over locations where there was a conversion from agricultural and pastureland to deciduous forest. The largest decreases in mean temperature (i.e., the darker blue shaded contours in Figure 7) resemble the locations of reforestation in Figure 4b.

[45] Considering that these differences reflect those temperature changes between the mean atmospheres for our two land cover cases, we evaluated the variability of the temperature differences between individual ensemble members. The temperature variation between these different member combinations is, in general, lower than the respective variation between our land cover data sets. This gives us additional confidence that the simulated temperature change that accompanies documented land cover change in our model is, in fact, robust. Figure 8 also indicates that the mean monthly temperature change between individual members (for example, the 1 July atmosphere with present-day land cover minus the 3 July atmosphere with historical land cover, as shown in Figure 8b) are generally similar to the corresponding temperature changes between old and new land cover. Except for locations where there are distinct spatial changes in rainfall (e.g., central NJ in Figure 8g), we note that the temperature variation between different ensemble combinations for a given area or land cover tends to be smaller than the signal due to land cover change between past and present.

[46] The land cover changes have also influenced the simulated monthly mean daily maximum and minimum temperatures (Figure 9). In general, the patterns match those

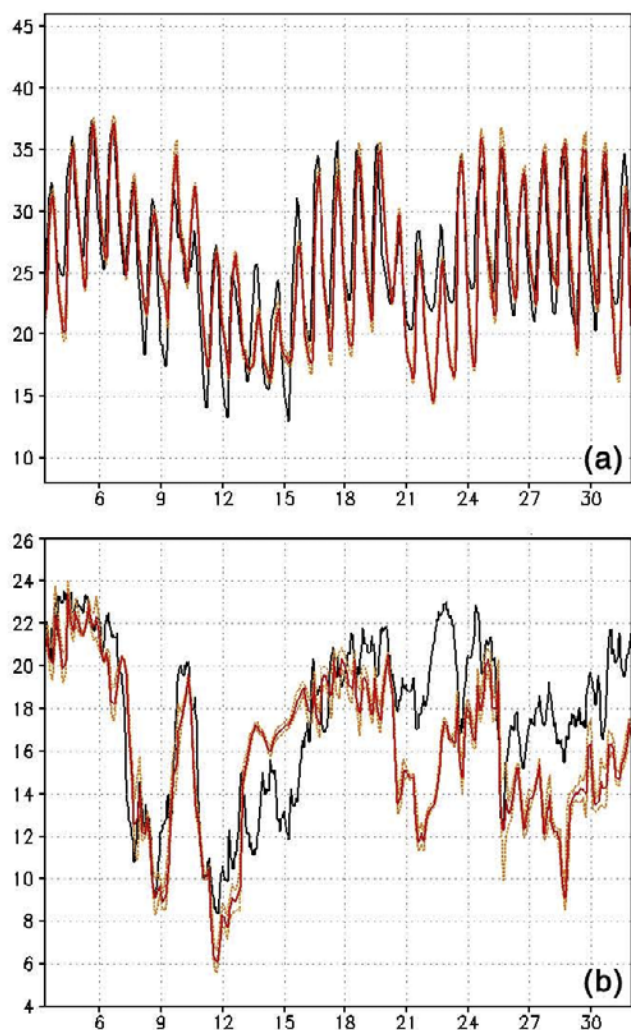


**Figure 6.** The time series of (a) observed hourly July surface air temperatures (black) and simulated temperatures from the control run ensemble (solid red), in degrees Celsius, and (b) observed July surface dew point temperatures (black) and simulated dew point temperatures from the control run ensemble (solid red), in degrees Celsius. In both panels, the time series represents temperatures that are averaged over the twelve noncoastal stations on grid 3. The  $x$  axis represents the day of July. For each panel, the  $\pm 1.0$  mean standard deviations of the individual ensemble members, added to the respective simulated values and also in degrees Celsius, are indicated by red dashed lines.

for the mean temperatures, but with more pronounced changes in the daily maximum temperature. In other words, the present-day landscape seems to be associated with a larger diurnal temperature range (DTR).

[47] This raises an interesting question: because urbanization is a large driver of our simulated temperature changes, why do we not see a decrease in DTR for the more urbanized, present-day landscape? For example, *Collatz et al.* [2000] and *Kalnay and Cai* [2003] suggest that the observed decreases in DTR are consistent with urbanization. In a physical sense, the urban heat island (UHI) phenomenon results from the combination of distinct effects of the urban

environment on air temperatures. First, the urban landscape, with its darker-colored roof structures and paving materials, can absorb a greater percentage of available incoming short-wave radiation compared to adjacent rural areas [*Taha, 1997*]. Simultaneously, the removal of vegetation shifts the surface energy partitioning into more sensible and less latent heat [*Chagnon, 1992*]. Both of these effects contribute to elevated daytime surface air temperatures, and, as will be discussed shortly, RAMS reproduces this expected behavior.

[48] In addition, however, the built-up areas have increased mass and thus increased heat storage [*Oke, 1982; Grimmond and Oke, 1999*]. Other effects, like anthropogenic energy releases [*Oke, 1988*] and air stagnation within urban canyons, also contribute. Observed nocturnal temperatures within these areas tend to cool much more gradually than they do within the less developed surroundings, often leading to a relative reduction in the DTR over the city. At this time, RAMS does not include these effects, resulting in a likely underestimate of the increase in daily minimum temperature in large urban regions of our model domain. Future versions of the LEAF land surface model will likely address some of these issues, for example, by including urban canopy heating terms like *Brown and Williams* [1998] and *Voogt and Oke* [1997], and assigning different roughness heights for levels of the urban hierarchy (e.g., town, city, metropolis). In addition, the vertical grid resolution of the lowest atmospheric layer of our model (i.e., 50 m) is a full order of magnitude lower than what *Pielke et al.* [2007] suggest is needed to properly reproduce observed nighttime temperature trends. Because nocturnal temperatures can be particularly sensitive to boundary layer variables such as wind speed, surface roughness, and soil heat capacity [*Shi et al., 2005*], the lack of high vertical grid resolutions on the order of 5 m or less can create additional uncertainties when modeling near-surface nighttime temperatures [*Pielke et al., 2007*]. As computing power increases, carrying out simulations with a full urban model coupled to RAMS, and also with a sufficiently high vertical grid resolution, is a promising avenue for future study.

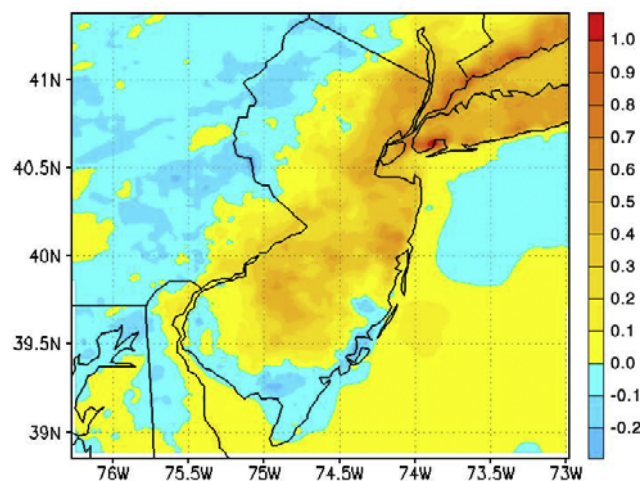


**Figure 7.** Mean monthly differences (present-day minus historical land cover), for July, of hourly RAMS air temperatures between the ensemble runs. The units are in degrees Celsius.

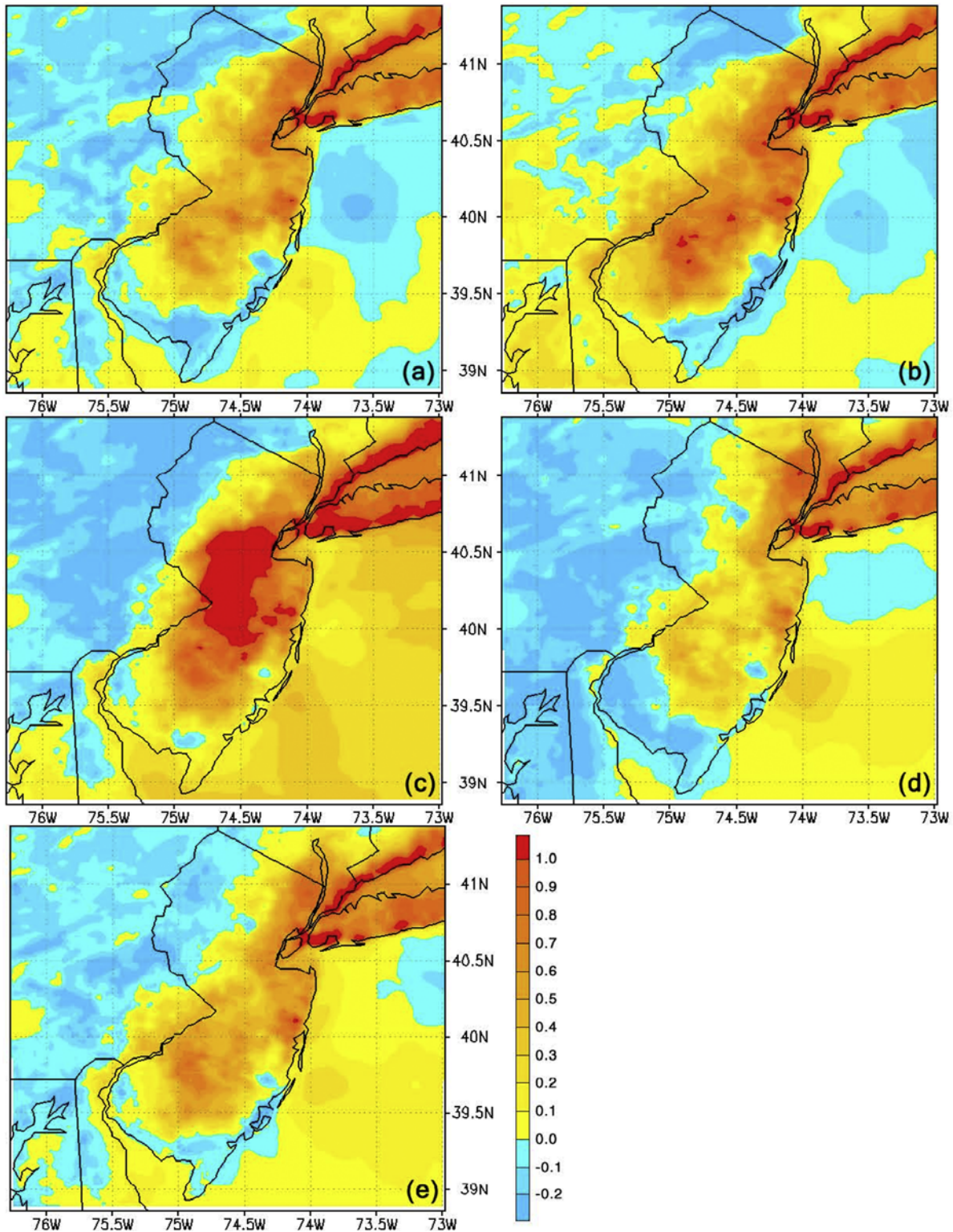


**Figure 8.** Mean monthly temperature differences, in degrees Celsius, between individual members of the historical and present-day ensembles. Each member is denoted by its initial atmosphere followed by an  $h$  for the run with historical land cover, and a  $p$  for the run with present-day land cover: (a) July $1p$  minus July $1h$ ; (b) July $1p$  minus July $3h$ ; (c) July $1p$  minus June $29h$ ; (d) July $3p$  minus July $1h$ ; (e) July $3p$  minus July $3h$ ; (f) July $3p$  minus June $29h$ ; (g) June $29p$  minus July $1h$ ; (h) June $29p$  minus July $3h$ ; and (i) June $29p$  minus June $29h$ .

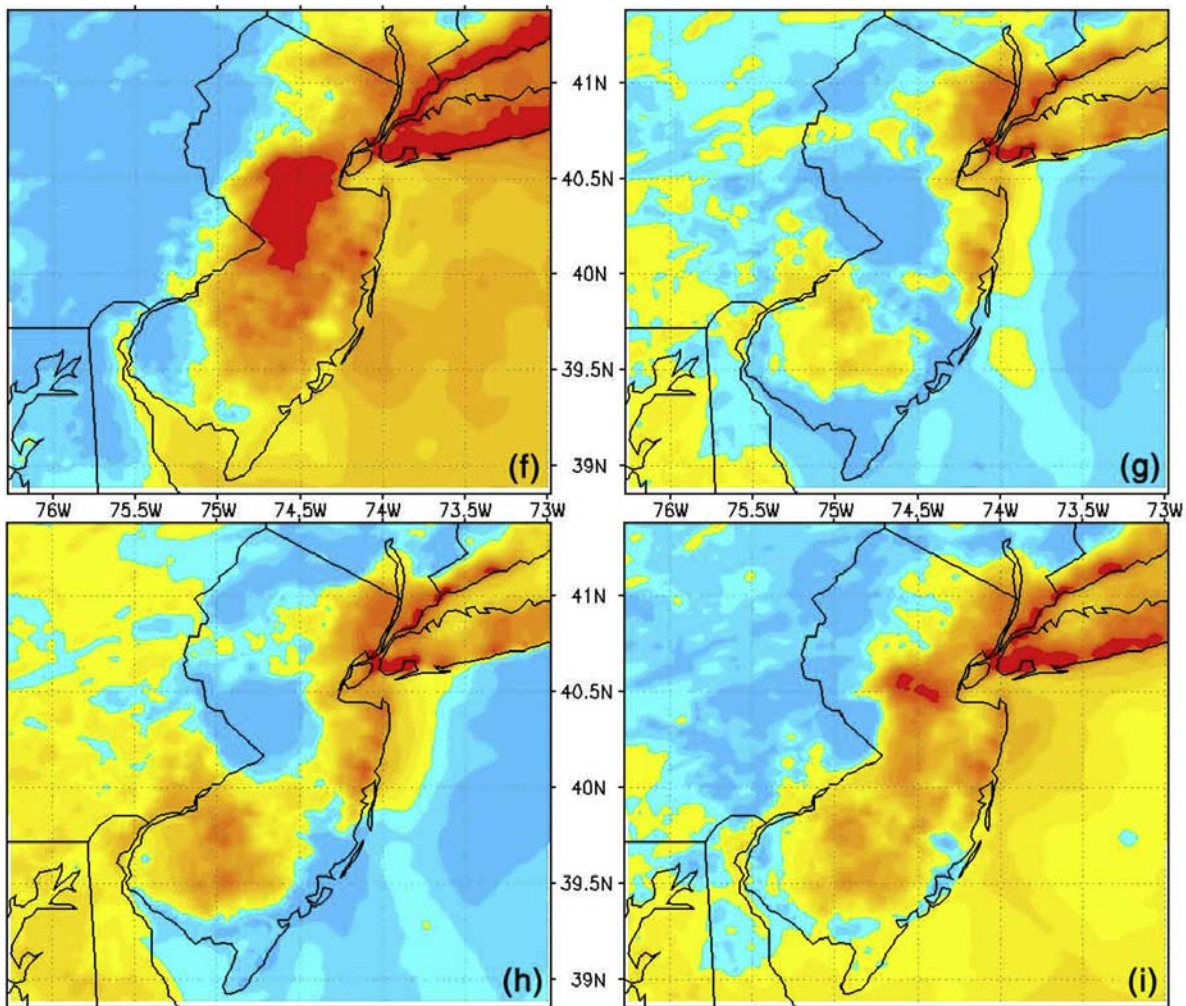


**Figure 8.** (continued)

[49] Figure 10 shows the monthly mean diurnal cycle of surface air temperature differences for all land surfaces and for the three LCC themes shown in Figure 4. Over all land surfaces, the peak warming of about  $0.2^{\circ}\text{C}$  lasts from locally late morning to early evening. These temperature differences decrease during the night to a minimum around sunrise. For the grid cells that have experienced urbanization (Figure 4a), the pattern is similar but with a much larger signal, e.g., a peak afternoon increase for the present-day landscape by about  $0.7^{\circ}\text{C}$ . Consistent with Figures 7 and 9, the reforested grid cells (Figure 4b) show slightly cooler temperatures throughout the day. Finally, the deforestation patches (Figure 4c) show a similar pattern to the urbanized areas, but with a slightly smaller amplitude.

### 3.3.2. Dew Point Temperatures

[50] Figure 11 shows the differences in mean July 1999 surface air dew point temperatures between our present-day and historical ensembles. The dew point decreases of  $0.3\text{--}0.6^{\circ}\text{C}$  within central and southern NJ suggest that the near-surface air over the present-day landscape is less humid. Together with the simulated increase in surface air temperatures, our first atmospheric model layer is warmer and drier for the present-day landscape. By

contrast, in the reforested areas of the domain, dew points are generally greater in the present-day ensemble.

[51] These general trends are consistent with the monthly mean diurnal cycle of dew point differences (Figure 12). Here, the grid cells where localized deforestation has occurred have greater peak dew point decreases than the urbanized grid cells ( $0.6^{\circ}\text{C}$  compared to  $0.4^{\circ}\text{C}$ ), in part because of the compensating effect of the larger temperature increases over present-day urban areas. The peak increase over the reforested grid cells is about  $0.3^{\circ}\text{C}$  during midafternoon.

[52] The dew point decreases between the individual ensemble members are also spatially consistent with these changes. When dew point differences were compared between various combinations of ensemble members, there was a persistent (and pronounced) dew point decrease in central and southern NJ. The overall pattern does increase the confidence in our results, but variations in monthly rainfall between the members can produce large spatial differences in dew points. Nevertheless, we find that the broad dew point changes that result from land cover change are reasonably robust. For a given land cover data set, monthly dew point values are all within  $0.1\text{--}0.3^{\circ}\text{C}$  for individual ensemble members, and like temperature, the

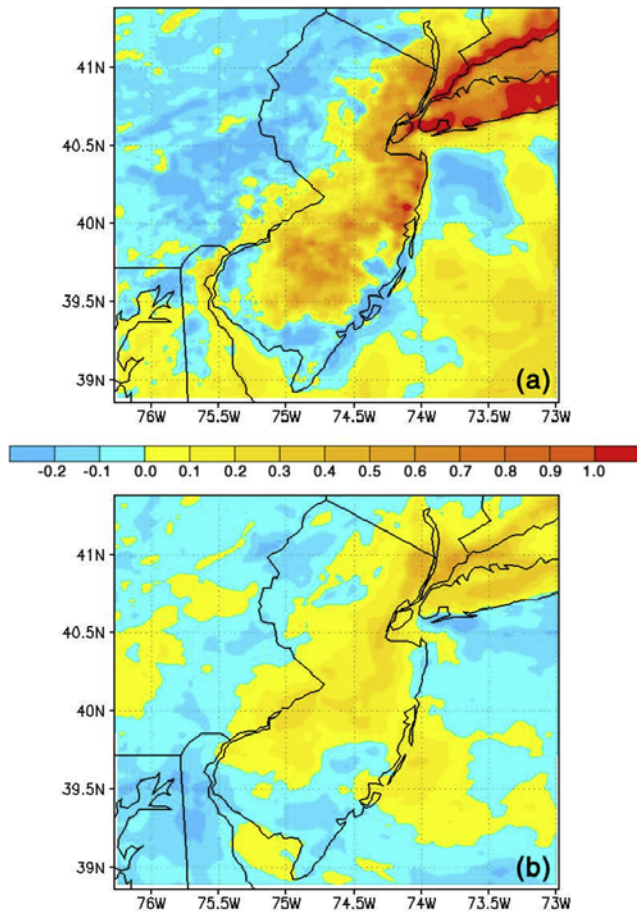


**Figure 9.** As in Figure 7 except for (a) daily maximum near-surface air temperatures and (b) daily minimum near-surface air temperatures. The units are in degrees Celsius.

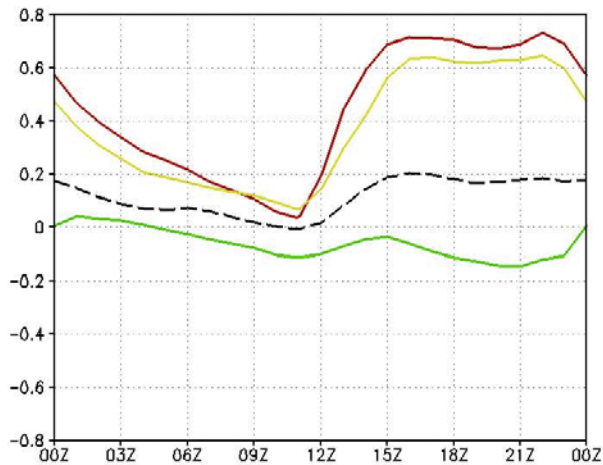


**Figure 10.** The diurnally averaged monthly time series of mean July near-surface air temperature differences (present-day minus historical land cover), in degrees Celsius, for those grid cells that have experienced a change in dominant land cover resulting from urbanization (red), reforestation (green), deforestation (yellow), and for all land points on grid 3 (dashed black). The  $x$  axis represents the hour of universal time.

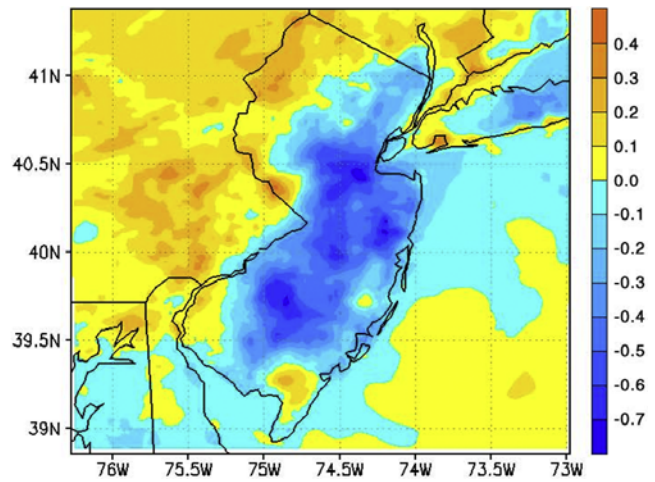


**Figure 11.** As in Figure 7 except for near-surface dew point temperatures. The units are in degrees Celsius. The contour interval for this figure has a different range than those of Figures 7–9.

standard deviations are slightly larger in magnitude for those grid cells that have been converted to urban land cover, while smaller standard deviations characterize the grid cells that have become reforested.

### 3.3.3. Rainfall

[53] Figure 13a illustrates the mean spatial differences in July rainfall totals for the period from 1200 UTC 3 July and 0400 UTC 1 August. The difference pattern is more or less random across the model domain, with patchy decreases and increases adjacent to each other. This suggests slight shifts in the convective triggering regions rather than systematic changes in rainfall. Consistent with this, the domain-averaged hourly rainfall rates and timing of individual rain events, as shown in Figure 13b, are similar in both ensembles.

[54] Figure 13b also shows that, for a given land cover data set, the domain-averaged +1.0 standard deviation between the individual ensemble members, added to the

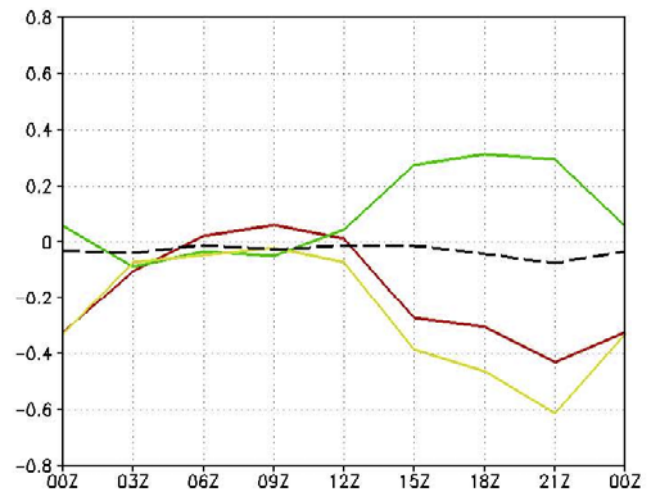


**Figure 12.** As in Figure 10 except for near-surface dew point temperatures.

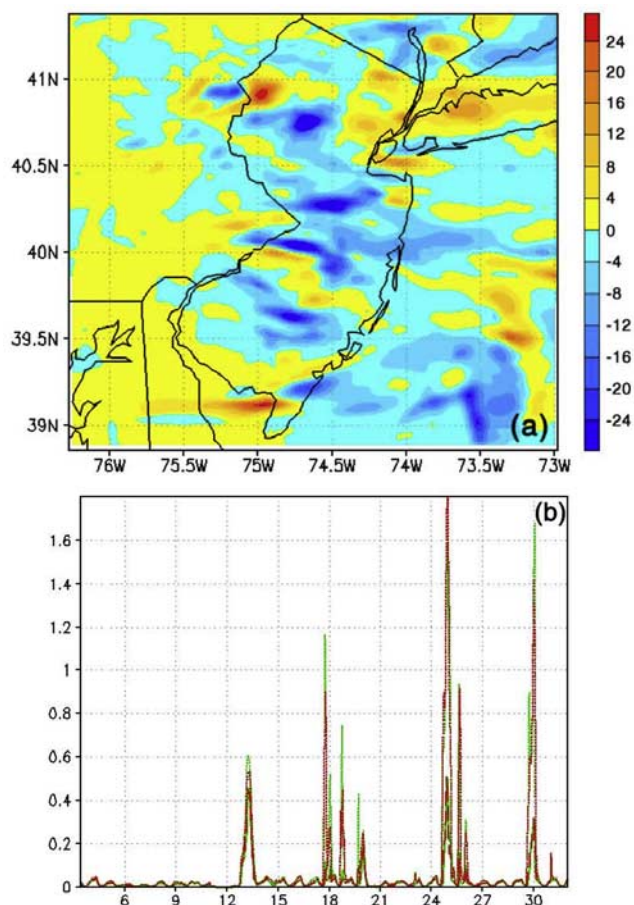


**Figure 13.** (a) Monthly mean differences (present-day minus historical land cover) in cumulative rainfall totals, in mm, extracted from the final time of the ensembles, at 0400 UTC 1 August, and (b) the domain-averaged monthly time series of mean rainfall intensity differences, in  $\text{mm h}^{-1}$ , of the ensemble with historical land cover (solid green) and with present-day land cover (solid red). The time series of the  $+1.0$  mean standard deviations of hourly rainfall rates, added to the respective mean ensemble values and in  $\text{mm h}^{-1}$ , are indicated by the dashed lines. The historical standard deviation is represented by the green dashed line, and the present-day standard deviation is represented by the red dashed line.

respective rainfall rate at each time step, can be quite large during the times of convective events. Thus, the variation of rainfall among the three ensemble members is approximately as large in magnitude as the variation of rainfall between the land cover cases. For instance, during the evening of 17 July, the 29 June ensemble member simulated an intense convective cell in which rainfall rates were  $7.0 \text{ mm h}^{-1}$  along the NJ/NY state border. At the same time, although a weaker ( $3.5 \text{ mm h}^{-1}$ ) and smaller convective cell developed in the 1 July ensemble member over the same region, there was virtually no convection that developed in the 3 July ensemble member around this location. These three runs had the same present-day land cover. The large differences in rainfall rates resulted in significant variations in total rainfall among the ensemble members for a given convec-

tive event. While this suggests that the changes in monthly rainfall amounts between our land cover cases are random and not statistically significant, it also implies that the changes in dew point temperatures between our ensembles can be highly dependent upon these random spatial differences in rainfall.

### 3.4. Simulated Differences in the Surface Energy Budget With Historical Versus Present-Day Landscapes

#### 3.4.1. Surface Albedo

[55] The changes in RAMS-calculated net broadband surface albedo between our present-day and historical ensembles, as shown in Figure 14, are generally consistent with the land cover changes we have described (see section 3.1). Urbanization has produced a strong albedo decrease in our model, which acts as a positive radiative forcing on the surface energy budget. The urban class in LEAF-2 was defined using an estimated broadband surface albedo value of 0.15 which combines the albedos from both residential and traditional urban land cover types into a “harmonized” value representative of a combination of low-density residential, high-density residential, and urban built-up and commercial surfaces [Pielke, 2002; Offerle *et al.*, 2003]. Jin *et al.* [2005] also reported that urban areas have surface albedos that are lower than those of croplands and deciduous forests during summer. As we have documented, the conversion of the predominant 19th-century agricultural and forested landscape with urban areas resulted in decreased albedos in these regions, as well as decreased evapotranspiration (ET) rates due to reduced vegetation and a lower LAI. The decreased albedo and ET rates contributed to the well-defined urban warming that we have observed in our present-day simulations.

[56] Conversely, for reforested areas, the increases in albedo imply a negative radiative forcing that contributes to the cooling of the present-day landscape. For instance, the pine forested region that historically dominated parts of coastal central NJ has likely trended toward a combination of deciduous broadleaf forest and mixed forest during the 20th century. Further to the north, within a broad region that includes central and south-central NJ, similar net albedo increases probably resulted from an increased deciduous component of the forest in addition to isolated increases in agricultural row crops and pastureland. The albedo increases are consistent with these land cover changes.

[57] This particularly fragmented albedo difference pattern characterizing this area of NJ is also associated with landscape heterogeneity due to a combination of land cover changes, including forest regrowth, isolated deforestation, limited agricultural expansion, and urbanization. Because increased fragmentation of the land surface can affect convection initiation and other land-atmosphere interactions, we examine the atmospheric effects of increased land surface heterogeneity in greater detail in our companion paper.

[58] While urban surfaces in our model have a lower albedo (0.15) compared with many vegetation types we have used in this study, including agriculture and pastureland (0.18) and deciduous forest (0.20), the urban land cover class in LEAF-2 also has a reduced vegetative component that results in a drier surface layer. Sensible heating is thus strong in the daytime, leading to pronounced

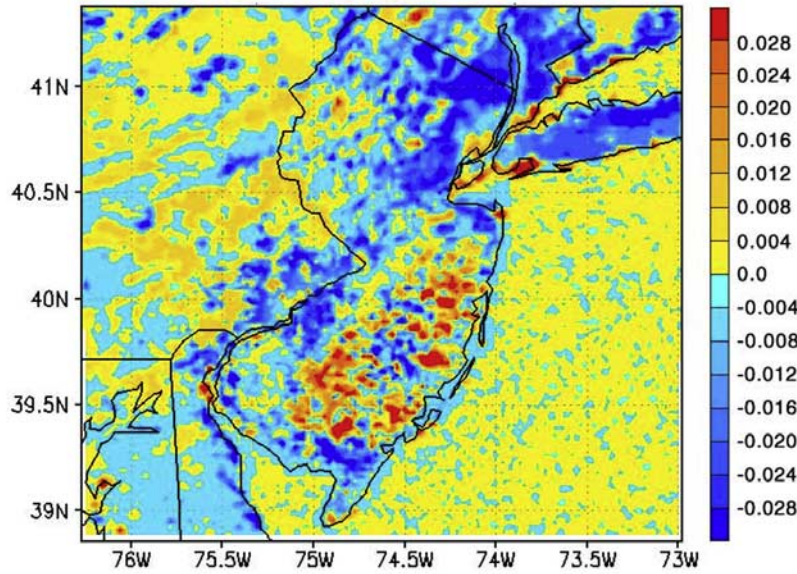


**Figure 14.** As in Figure 7 except for model-calculated net surface broadband albedo.

increases in maximum urban temperatures. These albedos, however, are not relevant during the nighttime hours, and with no representation of anthropogenic heat sources in LEAF-2, modeled nocturnal minimum temperatures are lower than observed values.

[59] The apparent surface albedo increases in central NJ demonstrate that land use practices can alter the radiative energy balance. As we show in the following sections, the removal of the forest canopy shifts the radiative partitioning toward sensible heat flux that warms the overlying air. While the radiative energy balance on local and regional scales can be modified by changes in albedo, it is the changes to the surface thermal and moisture characteristics resulting from LULCC, in this case deforestation, that can alter the partitioning of net shortwave radiation between sensible and latent heat flux.

### 3.4.2. Surface Heat Fluxes

[60] We consider the energy balance of the surface, defined here to consist of the top layer of soil (5 cm thick in this study), vegetation, and the air within the depth of the vegetation. The net sensible and latent flux leaving this surface is given by:

$$Q_N = Q_H + Q_E + Q_G \quad (1)$$

where  $Q_H$  is the turbulent sensible heat flux to the atmosphere,  $Q_E$  the turbulent latent heat flux to the atmosphere, and  $Q_G$  the sensible heat flux to deeper soil layers. The flux  $Q_G$  is a relatively small percentage, generally 10% or less, of  $Q_N$  when averaged over a diurnal cycle [Sellers *et al.*, 1997], so it is considered negligible in this analysis.

[61] The net radiative flux received at the land surface  $R_N$  is defined by:

$$R_N = R_{SW\downarrow} - R_{SW\uparrow} + R_{LW\downarrow} - R_{LW\uparrow} \quad (2)$$

where  $R_{SW\downarrow}$  and  $R_{LW\downarrow}$  are the downward shortwave and longwave radiative flux components, respectively, that are

incident on the land surface;  $R_{SW\uparrow}$  is the reflected flux of shortwave radiation; and  $R_{LW\uparrow}$  is the upward flux of longwave terrestrial radiation. To further simplify our discussion, we define  $R_{SW}$  (note the absence of an arrow in the subscript) as the difference between the incoming and reflected fluxes of solar radiation, and likewise,  $R_{LW}$  as the difference between the downward flux of longwave radiation and the terrestrial flux emitted by the surface to the atmosphere. Equation (2) shows that the sum of  $R_{SW}$  and  $R_{LW}$  is equivalent to the total net radiation received at the land surface.

[62] Mean monthly differences in sensible and latent heat fluxes are shown in Figure 15. Figure 15a indicates that  $Q_H$  has increased by 10–30  $\text{W m}^{-2}$  within the areas where mean temperatures have warmed in our present-day ensemble. However,  $Q_E$  has decreased over the present-day landscape in these same regions, as shown in Figure 14b. The monthly area-averaged trends of these fluxes (not shown) show an overall increase in  $Q_H$  with a decrease in  $Q_E$ . In fact, between 3 July and 31 July, the mean area-averaged daily  $Q_H$  in both ensembles increased by about 65  $\text{W m}^{-2}$  (i.e., an estimated 105% increase), as the daily area-averaged  $Q_E$  sharply declined by 80  $\text{W m}^{-2}$  but remained positive at the end of the month (i.e., an estimated 65% decrease). These general trends match up reasonably well for those grid cells where urbanization and localized deforestation have occurred. The enhanced  $Q_H$  is also consistent with the lack of significant monthly regional rainfall totals simulated by our model.

[63] The mean diurnal cycle of heat flux differences for each of our LCC themes are shown in Figure 16. We supplement Figure 16 with Table 4, which lists the monthly mean percentage change in each of the heat and radiative flux components at 1800 UTC local time (i.e., close to the time of maximum surface heating), together with the respective percentage changes in  $Q_N$  and  $R_N$ . These percentage changes, however, do not represent absolute changes in  $\text{W m}^{-2}$ .

[64] Over all present-day land surfaces, there has been minimal change in the intensity of these heat fluxes over the

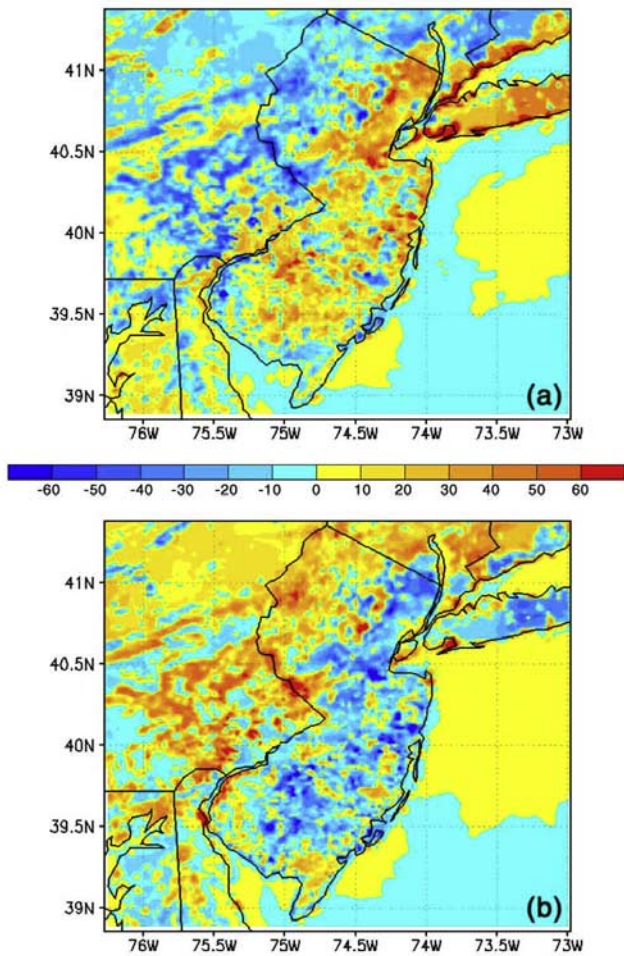


**Figure 15.** As in Figure 7 except for (a) surface sensible heat flux and (b) surface latent heat flux. The units are in  $W m^{-2}$ .

diurnal cycle, aside from a small positive increase in  $Q_N$  during the afternoon (3.6%). The conversion to urban land cover produces a large change in these heat fluxes.  $Q_H$  increases over the present-day urban landscape by an estimated 25% during the early afternoon with a reduction of  $Q_E$  by 24% (see Figures 16a and 16b). These changes are consistent with the decreases in surface albedo we have described earlier (Figure 14). We also note that *Adegoke and Gallo* [2006] produced similar trends in  $Q_H$  and  $Q_E$  with their LULCC sensitivity study of the urban Baltimore-Washington DC area. Reforestation, however, produces the opposite effect, decreasing  $Q_H$  while increasing  $Q_E$ . Figure 16c shows that upward turbulent energy flux over these reforested areas can increase by  $30 W m^{-2}$  for the present-day landscape. This is very similar to the peak increases over present-day urban regions, but unlike the urbanization LCC, the contribution is due to enhanced heating latent

[65] For our localized deforestation patches, the peak increase in  $Q_H$  during the afternoon is very close in magnitude to the increase over urbanized areas. However, because of the sharper decline in  $Q_E$  over these deforested grid cells, the change in  $Q_N$  becomes weakly negative during the time of maximum surface heating (Figure 16c).

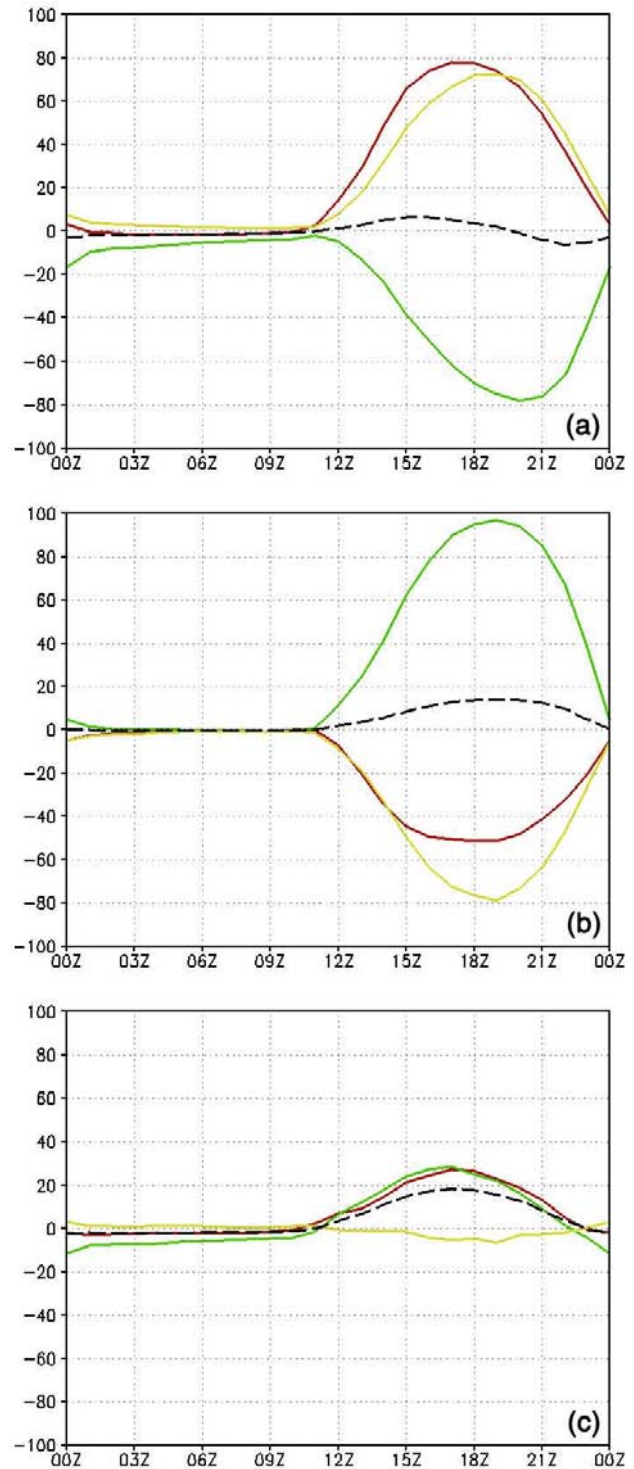


**Figure 16.** The diurnally averaged monthly time series of differences (present-day minus historical land cover) in (a) surface sensible heat flux, (b) latent heat flux (b), and (c) net sensible and latent heat flux, for those grid cells that have experienced a change in dominant land cover resulting from urbanization (red), reforestation (green), deforestation (yellow), and for all land points on grid 3 (dashed black). The units in all panels are in  $W m^{-2}$ .

**Table 4.** Monthly Mean Percentage Change in Surface Heat and Radiative Flux Components<sup>a</sup>

	$Q_H$	$Q_E$	$Q_N$	$R_{SW}$	$R_{LW}$	$R_N$
All land points	1.2	7.5	3.6	0.3	1.8	0.8
Urbanization	25.4	-24.7	5.2	2.4	2.4	3.5
Reforestation	-19.8	63.4	5.0	-0.4	8.1	1.5
Deforestation	29.6	-25.6	-0.8	1.5	-4.6	0.8

<sup>a</sup>These values represent the monthly mean percentage change (i.e., present-day land cover minus historical land cover), both for all land points and for each of the land cover conversions, in the surface heat and radiative flux components. These percentages are relative to 100%, and are each valid at 1800 UTC local time.

This decrease in  $Q_N$  does not necessarily imply that the present-day ensemble atmosphere would be cooler, because horizontal and vertical advective and turbulent heat mixing within the atmosphere, as well as direct radiative heating of the atmosphere, are other pathways that can also warm or cool air temperatures.

### 3.4.3. Surface Radiative Fluxes

[66] Mean monthly differences in  $R_{SW}$ , as shown in Figure 17a, suggest that the present-day landscape has received, in general, about 4–10  $W m^{-2}$  more net shortwave radiative flux compared to the historical landscape. These changes are also positive for nearly the entire state of NJ. The increases in  $R_{SW}$  for the present-day landscape imply that more sunlight reaches the surface, especially within urban locations in NY and NJ. These are areas that have experienced strong albedo decreases, enhanced warming of air temperatures, and modest dew point declines.

[67] There are even stronger increases in  $R_{SW}$  over some isolated areas of southern NJ in the same locations where our land cover data sets suggest a conversion from mixed forest to pine forest. In this region centered on 39.7°N and 74.6°W, the resulting forest species change allows 10–16  $W m^{-2}$  more net shortwave radiation to be received by the land surface in our present-day ensemble. There is also an accompanying 0.4–0.8°C warming of present-day soil temperatures within this same region (for the four soil layers above a 30 cm depth), with smaller temperature increases still evident within deeper soil layers.

[68] Conversely, for those areas of eastern PA that have become reforested,  $R_{SW}$  has decreased by 4–6  $W m^{-2}$  with stronger radiative decreases over some of the more densely reforested areas. The conversion from agricultural and pastureland to deciduous forest in these regions has increased the LEAF-2 surface albedo from 0.18 to 0.20 while also enhancing ET rates due to greater rooting depths. This is consistent with the 0.8–1.0°C cooling of the four topmost soil layers in these regions in our present-day ensemble (not shown). In our companion paper, we investigate the physical mechanisms in RAMS, such as enhanced cloudiness and/or increased atmospheric water vapor content, which are likely associated with these  $R_{SW}$  decreases.

[69] The mean monthly differences in  $R_{LW}$  between our simulations are shown in Figure 17b and in Table 4. Figure 17b reveals little, if any, variation in  $R_{LW}$  that results from urbanization. The significant changes in  $R_{LW}$  appear to be related to changes in forest cover or composition. If the present-day landscape becomes reforested,

which has occurred in the northern and western sections of our domain,  $R_{LW}$  generally increases. However, if the land cover changes trend toward an increased deciduousness, as in central and southern NJ,  $R_{LW}$  declines.

[70] The differences in  $R_{LW}$  between our ensembles can also be induced by a combination of changes to the land surface and the atmosphere, which can, in effect, modulate the upward and downward fluxes of longwave radiation. These differences in  $R_{LW\uparrow}$  are generally consistent with the changes in surface temperatures between our ensembles and also differences between model emissivity values that can occur because of historical land cover shifts within a grid cell. The differences in  $R_{LW\downarrow}$  are, however, due solely to changes in atmospheric conditions, such as differences in cloudiness, air temperature, or air humidity. The modeled decreases in  $R_{LW\downarrow}$  are particularly evident near the central NJ coast where daily maximum temperatures over land have warmed by 1.0°C and surface air humidity fractions have also declined by 0.03. In effect, the change in  $R_{LW\uparrow}$  is amplified relative to the changes in  $R_{LW\downarrow}$ , suggesting that the change in surface conditions has a more significant influence on longwave radiative flux than the change in atmospheric conditions that result from land cover change.

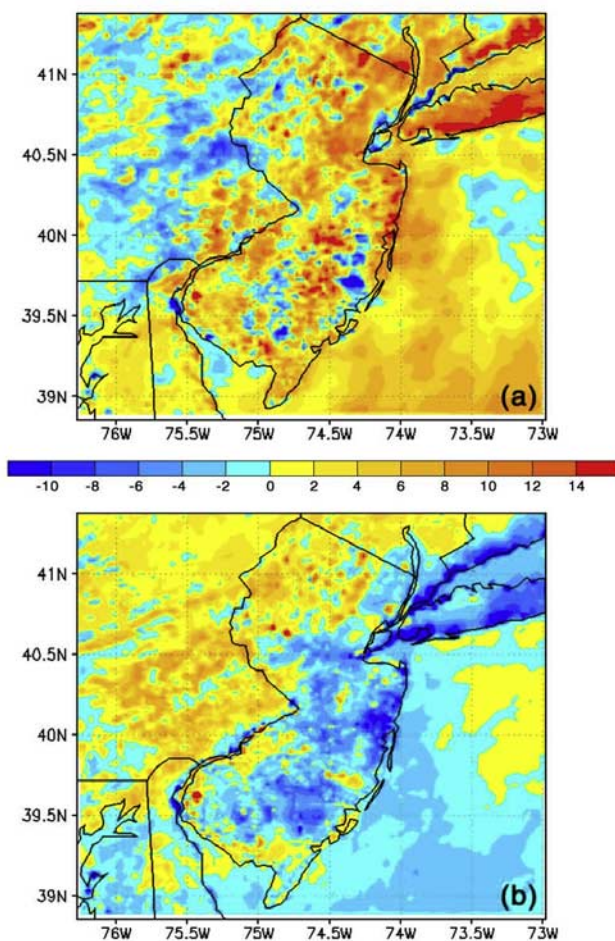


**Figure 17.** As in Figure 7 except for (a) net downward shortwave radiative flux and (b) net downward longwave radiative flux. The units are in  $W m^{-2}$ .

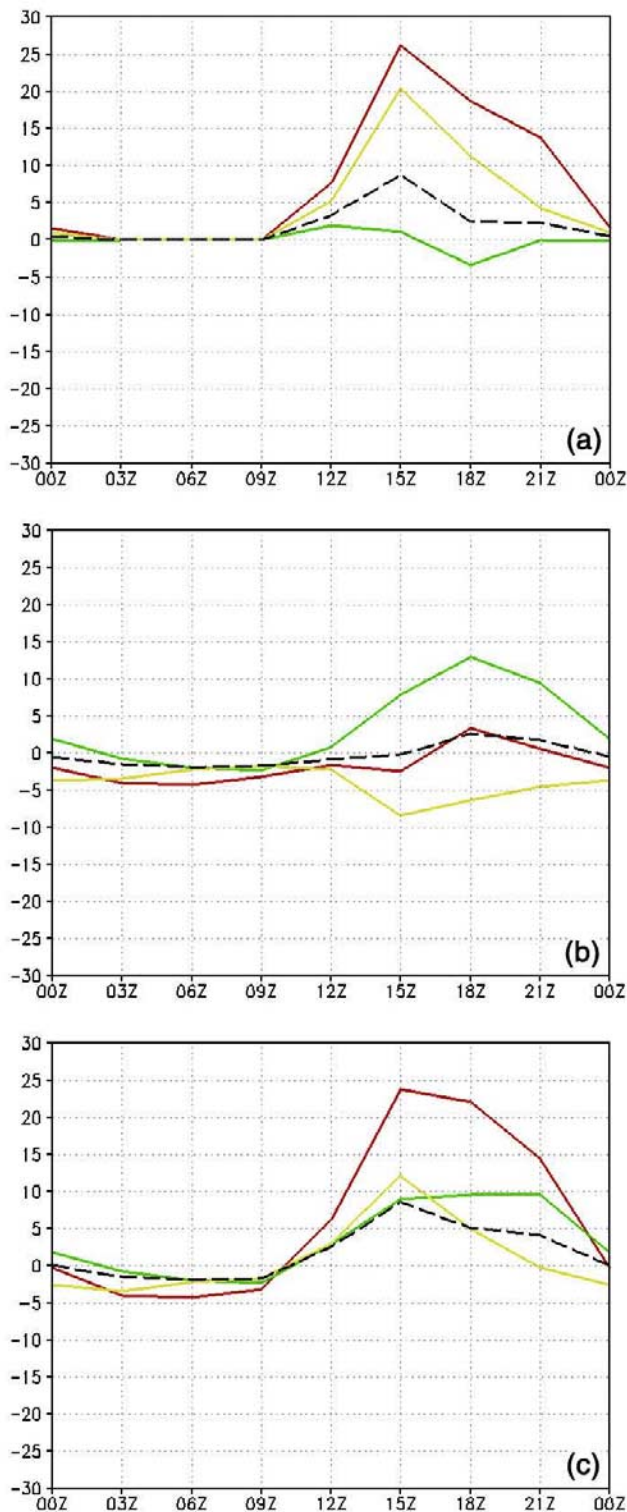


**Figure 18.** As in Figure 16 except for the differences in (a) net downward shortwave radiative flux, (b) net downward longwave radiative flux, and (c) total net radiative flux received by the surface. The units in all panels are in  $\text{W m}^{-2}$ .

[71] The mean diurnally averaged changes in  $R_{SW}$  and  $R_{LW}$  for each of our LCC themes are shown in Figures 18a and 18b, respectively, with the trends in total radiative flux  $R_N$  summarized in Figure 18c. While the conversion to

urban land cover has produced relatively strong increases in  $R_{SW}$  during the morning hours following sunrise, there were little, if any, diurnal changes in  $R_{LW}$  in our simulations. As a result, the diurnal increases in  $R_N$  (maximizing at  $25 \text{ W m}^{-2}$ ) within urban areas resembled the corresponding trend in  $R_{SW}$ . The urbanization and deforestation LCCs also have relatively similar diurnal increases in  $R_{SW}$ .

[72] Throughout this paper, we have described the ways in which historical land cover change can modify the properties of the land surface, consequently altering the key components of the surface energy balance that control processes at the land surface-atmospheric boundary. Urbanization has significantly warmed the land surface via strong decreases in albedo and increases in net shortwave radiation, both of which may have enhanced sensible heat flux by as much as 25% by early afternoon. However, reforestation (i.e., the conversion of agricultural and pastureland to deciduous forest) has generally increased surface albedo and reduced net incoming shortwave radiation, enhanced ET rates, and cooled surface air temperatures. The surface energy budget has also been strongly influenced by the potential changes in forest composition within central and southern NJ, where an increase in forest deciduousness, combined with isolated increases in agricultural and pastureland, may have enhanced surface albedo and decreased net shortwave and net downward longwave radiative flux. Over deforested regions, the repartitioning toward sensible heat flux with reduced ET rates has likely warmed daytime air temperatures and decreased dew points.

#### 4. Conclusions

[73] We have performed a sensitivity experiment which complements recent LULCC studies such as those by *Pielke et al.* [1999], *Mölders* [2000], *Marshall et al.* [2004a, 2004b], and *Schneider et al.* [2004]. Each of these studies used mesoscale models and sensitivity analysis to quantify the potential effects of land use change on regional weather and climate. In our study, we have documented the change in land cover within NJ and its surrounding states from a predominantly agrarian landscape to a heterogeneous mosaic of forests, farms, and urban areas over a roughly century-long time period.

[74] These land cover changes can be categorized according to three trends that have occurred since the late 19th century: urbanization, reforestation, and isolated deforestation. Urbanization has occurred in areas of central and northeastern NJ, LI, and in southeastern PA, and has been generally associated with the loss of prime agricultural land and an expansion of impervious surfaces. Further to the north and west, from southeastern PA into northern NJ, the abandonment of 19th-century agricultural land use practices, combined with selective timber harvesting, has likely led to a broad reforestation of this region. In addition, localized deforestation has also occurred in southern NJ and LI. Accompanying all these conversions, the regional landscape has become increasingly fragmented and spatially heterogeneous.

[75] The historical and present-day landscape reconstructions that document these trends were used in the RAMS model, at a grid cell size of 2 km, to evaluate the sensitivity of changes in land cover on its weather and climate for July

1999 drought conditions. Ensembles of three simulations each were carried out for both the historical and present-day land cover conditions. For the present-day landscape, many regions that have experienced urbanization or deforestation have higher surface air temperatures combined with lower dew points in our model, suggesting warmer and drier near-surface air. Potential shifts in forest composition and rainfall differences may also have contributed to the dew point declines. The diurnal cycle of surface air temperature and dew point differences between our present-day and historical simulations are consistent with these trends. Differences between the individual ensemble members are, in general, similar to those between the ensemble means, though the use of ensembles helps to smooth the variability associated with convective rainfall that can have pronounced effects on surface temperature, dew point, and surface heat and radiative fluxes.

[76] Daytime maximum temperatures over the present-day urban landscape also increased considerably more than nighttime minimum temperatures in our simulations, suggesting an enhanced DTR. The warming of nighttime minimum temperatures within these present-day urban areas was likely underestimated in RAMS because the LEAF-2 parameterization does not yet account for the increased thermal and radiative properties of urban surfaces that contribute to anthropogenic energy storage and release. Future versions of LEAF-2 will likely include this effect.

[77] The responses of air and dew point temperatures suggest that land cover type can significantly modulate surface albedo and other key components of the land surface energy budget. Surface albedos have significantly declined in present-day urban regions. However, within central and southern NJ, the large patchy increases and decreases in surface albedo are due primarily to an overall increased deciduousness of its land cover in combination with local changes in forest composition, the regeneration of vegetation associated with disturbance, isolated patches of increased agricultural and pastureland, and forested wetlands change. Together, these conversions within a small region have increasingly fragmented the 19th-century landscape and imply that the present-day surface energy budget is more heterogeneous.

[78] These albedo changes also modify the partitioning of radiative energy into sensible and latent heat fluxes, which can directly affect air temperature increases or decreases. Sensible heat flux has increased where the present-day landscape has warmed. The present-day landscape receives more net shortwave radiation compared to the historical landscape, a trend that is consistent for nearly the entire state of NJ. Over reforested areas, net longwave fluxes have noticeably increased, with the largest increases during the afternoon hours. In addition, our study suggests that a change in land cover type, and the associated change in surface properties, has a more significant influence on net longwave radiative fluxes than does the corresponding change in atmospheric conditions that results from land cover change.

[79] The landscape change that we have observed over historical time is expected to continue and even accelerate into the future, driven primarily by the effects of a rapidly growing world population and the anthropogenic pressures exerted on natural environmental and ecological systems.

The northeastern U.S., in particular, was a very rapidly growing region of the world during the time period of this study (i.e., 20th century), and we have documented the extensive shifts from a predominantly agricultural landscape to a highly urban one within a relatively short time period. Our climate sensitivity analysis, even with the lack of an interactive urban model (which likely make our results a conservative estimate of the effects of LULCC on climate in this region), suggests that historical LULCC has the potential to modify surface properties with pronounced impacts on weather and climate, perhaps similar in magnitude regionally to those associated with increasing greenhouse gas concentrations [*Intergovernmental Panel on Climate Change*, 2007]. These findings are consistent with recent suggestions that assessing the full anthropogenic impact on the climate system will require expanded definitions of what constitutes “climate forcing” [*National Research Council*, 2005].

[80] On the basis of an extrapolation of the land cover trends identified in our study, what are some of the changes that we could anticipate in this region, perhaps 100 years from now? As a broad estimate, we expect urbanization to continue to expand outward from the two large metropolitan areas, consuming even more agricultural and pastureland within NJ and its adjacent states. We also expect reforestation rates to drop, as any abandoned agricultural land is more likely in the future to be converted to urban and commercial use. Deforestation rates and wetlands losses may decline, because of the continued enforcement of strict environmental laws and wetlands preservation. In light of these possible changes and the results of our simulations, we can anticipate that the future landscape will likely be warmer and drier than today.

## Appendix A: Supplementary Information for Land Cover Reconstructions

### A1. COOK Map Series

[81] The Cook map series has detailed land cover classes for the forests and wetlands within the state of NJ, as shown in Table 1. However, the map legend was incomplete and required some interpretation of forest types that were not explicitly identified. We interpreted regions of southern NJ that were depicted with asterisk-shaped symbols to be evergreen needleleaf forest, since these same symbols located within wetlands were clearly labeled as pine swamps. There were other, also apparently forested, areas with numerous cloud-shaped symbols that resembled the crown of a broadleaf deciduous tree; we interpreted these symbols as a deciduous forest cover type. Where these two symbols were numerous and evenly distributed, we assumed a mixed forest of evergreen and deciduous trees. The locations of deciduous, evergreen, and mixed forest types as we identified them are generally consistent with the distribution of these same forest types on a potential natural vegetation map for this region [*Kuchler*, 1964]. In addition, the general locations of the forests also correspond to those of present-day forest types as determined from recent Landsat imagery [*Vogelmann et al.*, 2001].

[82] We used a three-step process to determine the fractional percentages of other historical land cover categories

that were not explicitly mapped, including urban areas, pastureland, and mixed agricultural regions. First, we interpreted the extent of urban areas within NJ, and surrounding cities, such as New York and Philadelphia, from the coverage and density of the full road and rail network delineated on each map. Second, we interpreted a map symbol that resembled a few vertical blades of grass as pastureland or open areas dominated by grasses. Some of these areas closely correspond with the distribution of present-day pastureland. Finally, mixed agricultural land was then estimated on the basis of residual fractional percentages within each grid cell once all other types were identified, a reasonable assumption because agriculture is known to have been a dominant land cover type in 19th-century NJ. The validity of this approach was demonstrated by the favorable comparison between our derived estimates and the large fractional percentages of improved agriculture in many NJ counties as documented in the 1880 U.S. Census, as well as from personal communications with county historical commissions across the state. To minimize potential uncertainty, we took the additional step of merging the mixed agriculture and pastureland data for each grid cell and averaging their respective biophysical properties (e.g., surface albedo, roughness, displacement heights) in our land surface model. The merging of these two land cover types is reasonable because their biophysical properties tend to be very similar during the growing season, especially relative to the biophysical properties of the other land cover classes we have used in this study.

## A2. The 1880 U.S. Census Data

[83] We applied some adjustments and reconciliations to the census-based reconstruction based upon what is known about 19th-century land cover in the states surrounding NJ. The “other” nonfarmland category, by default, was assumed to correspond primarily to urban regions, because it was most commonly associated with the locations of known villages and cities. However, in some cases, we assigned a different land cover class where urban land cover was not reasonably consistent with known historical land use. For example, the original forests that covered parts of eastern PA and NY were repeatedly cleared or logged throughout most of the 1800s to support the demand for wood products for the lumber, fuel for heating, charcoal, and agriculture industries [Dowhan *et al.*, 1997]. By the late 19th century, the barren landscape had regenerated to short scrub oak with a mixed forest component. Since many of the grid cells with this “other” land cover class also covered a small fraction of total grid area, generally 10% or less, we reclassified the “other” land cover type within these cells to either deciduous forest or mixed agricultural land in the census data set. Similar land cover adjustments were necessary within the eastern half of LI, in DE, and throughout CT.

## Appendix B: Modifications to Land Cover Types in LEAF-2

[84] When preparing our surface data sets, we made two modifications to the land cover types in LEAF-2. First, to account for the regrowth of 19th- and 20th-century mixed forests that have occurred in the eastern U.S., we lowered

the displacement height for the LEAF-2 mixed forest class by 5.0 m in both land cover data sets. This helped to maintain continuity with the displacement height of the evergreen forests that characterize the Pine Barrens, which are scattered among the mixed forests of southern NJ. The 15.0 m displacement height that we have assigned in LEAF-2 to the mixed forest class is consistent with the 11.0–15.0 m canopies of the pine-oak forests that are predominant in this region [McCormick and Jones, 1973].

[85] Since the forested wetlands of NJ are also generally located in the Pine Barrens, we specified this land cover type in LEAF-2 to be a mixture of 50% deciduous shrub and 50% of our modified mixed forest [Dowhan *et al.*, 1997]. This characterization is consistent with the lowland vegetation of the region, as McCormick [1979] and Olsson [1979] noted that the forests within these wetlands are usually interspersed among understory shrubs of red maple, scrub oaks, and other broadleaf species. The initial soil water content for these forested wetlands (and for nonforested wetlands as well) was initialized in LEAF-2 as fully saturated for all soil layers below a depth of 10 cm, and with 85% and 88% of full saturation ( $\sim 0.38 \text{ m}^3 \text{ m}^{-3}$  volumetric soil water content for the silt clay loam soil type used here) at the two topsoil layers (from the surface to a depth of 10 cm), with no standing water above the ground surface. This vertical profile of soil wetness reasonably describes the mean hydrology of the forested and nonforested wetlands of NJ during the warm season with little, if any, widespread aboveground inundation [McCormick, 1979]. We used the same initial wetland soil moisture conditions for both the historical and present-day simulations, which assumes that the depth of the groundwater table was the same in both periods, although empirical observations have suggested that this might not be true [Epstein, 2003; M. N. Demitroff, personal communication, 2004].

[86] Although there was also no change in the LEAF-2 rooting depth for the same tree species between the historical and present-day data sets, we noted differences in the rooting depth by tree species. The trees within deciduous and mixed forests in LEAF-2 had mean rooting depths of 200 cm, while the trees within evergreen forests had shallower rooting depths of 150 cm [McQuilkin, 1935; Little and Garrett, 1990]. Since observational studies like Rowe and Reimann [1961] found that vegetative rooting depth and other factors can influence evapotranspiration (ET) rates, we may expect a change in forest composition between the late 19th and 20th centuries in a given region to have concomitant effects on surface air and dew point temperatures.

[87] **Acknowledgments.** This research was sponsored by a grant from the New Jersey Agricultural Experiment Station (NJAES), as part of the 2001 NJAES Graduate Scholar Program. The research and preparation of this article has also been supported by a grant from the NASA Goddard Space Flight Center, Biospheric Sciences Branch, through their Landsat Data Continuity Mission project. We thank David Robinson and Peter Wacker for their knowledge of New Jersey land cover and James Irons for his support. Pamela J. Waisanen also provided us with U.S. Census data for 1880. Finally, we humbly extend an appreciation to George H. Cook and Cornelius C. Vermeule, because without their true commitment and dedication to mapping New Jersey in the late 19th century, our land cover change project would likely have proved much more difficult, if not impossible.

## References

- Adegoke, J. O., and K. P. Gallo (2006), On the relation between surface spatial heterogeneity and climate prediction: Insights from the integration of fine resolution satellite land information into mesoscale climate models, paper presented at 86th Annual Meeting, Am. Meteorol. Soc., Atlanta, Ga., 29 Jan. to 2 Feb.
- Agthe, D. E. (1964), A study of the effect of urbanization on agriculture in New Jersey, M.S. thesis, 59 pp., Rutgers Univ., New Brunswick, N. J.
- Alderman, D. R., Jr., M. S. Bumgardner, and J. E. Baumgras (2005), An assessment of the red maple resource in the northeastern United States, *Northern J. Appl. For.*, **22**, 181–189.
- Anderson, J. R., E. E. Hardy, J. T. Roach, and R. E. Witmer (1976), A land use and land cover classification system for use with remote sensor data, *U.S. Geol. Surv. Prof. Pap.* **964**, 28 pp.
- Anthes, R. A. (1984), Enhancement of convective precipitation by mesoscale variations in vegetative covering in semiarid regions, *J. Clim. Meteorol.*, **23**, 541–554, doi:10.1175/1520-0450(1984)023<0541:EOCPBM>2.0.CO;2.
- Arnfield, A. J. (2003), Two decades of urban climate research: A review of turbulence, exchanges of energy and water, and the urban heat island, *Int. J. Climatol.*, **23**, 1–26, doi:10.1002/joc.859.
- Arriitt, R. W., et al. (2004), Ensemble methods for seasonal limited area forecasts, paper presented at 20th Conference on Weather Analysis and Forecasting/16th Conference on Numerical Weather Prediction, Am. Meteorol. Soc., Seattle, Wash., 12–16 Jan.
- Avissar, R. (1996), Potential effects of vegetation on the urban thermal environment, *Atmos. Environ.*, **30**, 437–448, doi:10.1016/1352-2310(95)00013-5.
- Avissar, R., and Y. Liu (1996), Three-dimensional numerical study of shallow convective clouds and precipitation induced by land surface forcing, *J. Geophys. Res.*, **101**, 7499–7518, doi:10.1029/95JD03031.
- Avissar, R., and R. A. Pielke (1989), A parameterization of heterogeneous land surfaces for atmospheric numerical models and its impact on regional meteorology, *Mon. Weather Rev.*, **117**, 2113–2136, doi:10.1175/1520-0493(1989)117<2113:APOHLS>2.0.CO;2.
- Avissar, R., and T. Schmidt (1998), An evaluation of the scale at which ground-surface heat flux patchiness affects the convective boundary layer using large-eddy simulations, *J. Atmos. Sci.*, **55**, 2666–2689, doi:10.1175/1520-0469(1998)055<2666:AEOTSA>2.0.CO;2.
- Baidya Roy, S., and R. Avissar (2000), Scales of response of the convective boundary layer to land surface heterogeneity, *Geophys. Res. Lett.*, **27**, 533–536, doi:10.1029/1999GL010971.
- Baidya Roy, S., C. P. Weaver, D. S. Nolan, and R. Avissar (2003a), A preferred scale for landscape forced mesoscale circulations?, *J. Geophys. Res.*, **108**(D22), 8854, doi:10.1029/2002JD003097.
- Baidya Roy, S., G. C. Hurr, C. P. Weaver, and S. W. Pacala (2003b), Impact of historical land cover change on the July climate of the United States, *J. Geophys. Res.*, **108**(D24), 4793, doi:10.1029/2003JD003565.
- Balling, R. C., Jr. (1988), The climatic impact of a Sonoran vegetation discontinuity, *Clim. Change*, **13**, 99–109, doi:10.1007/BF00140163.
- Beltrán, A. (2005), Using a coupled atmospheric-biospheric modeling system (GERRAMS) to model the effects of land-use/land-cover changes on the near-surface atmosphere, Ph.D. dissertation, 186 pp., Colo. State Univ., Boulder.
- Betts, R. A. (2001), Biogeophysical impacts of land use on present-day climate: near-surface temperature change and radiative forcing, *Atmos. Sci. Lett.*, **2**, 39–51, doi:10.1006/asle.2001.0023.
- Boardman, J., and D. T. Favis-Mortlock (2001), How will future climate change and land-use change affect rates of erosion on agricultural land? paper presented at Soil Erosion Research for the 21st Century, Am. Soc. of Agric. and Biol. Eng., Honolulu, Hawaii, 3–5 Jan.
- Bonan, G. B. (1997), Effects of land use on the climate of the United States, *Clim. Change*, **37**, 449–486, doi:10.1023/A:1005305708775.
- Bornstein, R., and Q. Lin (2000), Urban heat islands and summertime convective thunderstorms in Atlanta: three case studies, *Atmos. Environ.*, **34**, 507–516, doi:10.1016/S1352-2310(99)00374-X.
- Bounoua, L., G. J. Collatz, S. O. Los, P. J. Sellers, D. A. Dazlich, C. J. Tucker, and D. A. Randall (2000), Sensitivity of climate to changes in NDVI, *J. Clim.*, **13**, 2277–2292, doi:10.1175/1520-0442(2000)013<2277:SOCTCI>2.0.CO;2.
- Bounoua, L., R. Devries, G. J. Collatz, P. J. Sellers, and H. Kahn (2002), Effects of land cover conversion on surface climate, *Clim. Change*, **52**, 29–64, doi:10.1023/A:1013051420309.
- Brown, M. E., and D. L. Arnold (1998), Land-surface-atmosphere interactions associated with deep convection in Illinois, *Int. J. Climatol.*, **18**, 1637–1653, doi:10.1002/(SICI)1097-0088(199812)18:15<1637::AID-JOC336>3.0.CO;2-U.
- Brown, M., and M. Williams (1998), An urban canopy parameterization for mesoscale meteorological models, paper presented at 2nd Urban Environment Symposium, Am. Meteorol. Soc., Albuquerque, N. M., 2–6 Nov.
- Bryant, N. A., L. F. Johnson, A. J. Brazel, R. C. Balling, C. F. Hutchinson, and L. R. Beck (1990), Measuring the effect of overgrazing in the Sonoran desert, *Clim. Change*, **17**, 243–264, doi:10.1007/BF00138370.
- Chagnon, F. J. F., and R. L. Bras (2005), Contemporary climate change in the Amazon, *Geophys. Res. Lett.*, **32**, L13703, doi:10.1029/2005GL022722.
- Chagnon, F. J. F., R. L. Bras, and J. Wang (2004), Climatic shift in patterns of shallow clouds over the Amazon, *Geophys. Res. Lett.*, **31**, L24212, doi:10.1029/2004GL021188.
- Chagnon, S. A. (1992), Inadvertent weather modification in urban areas: Lessons for global climate change, *Bull. Am. Meteorol. Soc.*, **73**, 619–627, doi:10.1175/1520-0477(1992)073<0619:IWMIUA>2.0.CO;2.
- Chase, T. N., R. A. Pielke Sr., T. G. F. Kittel, R. Nemani, and S. W. Running (1996), Sensitivity of a general circulation model to global changes in leaf area index, *J. Geophys. Res.*, **101**, 7393–7408, doi:10.1029/95JD02417.
- Claussen, M., V. Brovkin, and A. Ganopolski (2001), Biogeophysical versus biogeochemical feedbacks of large-scale land cover change, *Geophys. Res. Lett.*, **28**, 1011–1014, doi:10.1029/2000GL012471.
- Collatz, G. J., L. Bounoua, S. O. Los, D. A. Randall, I. Y. Fung, and P. J. Sellers (2000), A mechanism for the influence of vegetation on the response of the diurnal temperature range to changing climate, *Geophys. Res. Lett.*, **27**, 3381–3384, doi:10.1029/1999GL010947.
- Copeland, J. H., R. A. Pielke, and T. G. F. Kittel (1996), Potential climatic impacts of vegetation change: A regional modeling study, *J. Geophys. Res.*, **101**, 7409–7418, doi:10.1029/95JD02676.
- Cotton, W. R., et al. (2003), RAMS 2001: Current status and future directions, *Meteorol. Atmos. Phys.*, **82**, 5–29, doi:10.1007/s00703-001-0584-9.
- Cunningham, J. T. (1981), New Jersey's rich harvest: A brief history of agriculture in New Jersey, 29 pp., N. J. Agric. Soc., Trenton.
- Cutrim, E., D. W. Martin, and R. Rabin (1995), Enhancement of cumulus clouds over deforested lands in Amazonia, *Bull. Am. Meteorol. Soc.*, **76**, 1801–1805, doi:10.1175/1520-0477(1995)076<1801:EOCOD>2.0.CO;2.
- Dickinson, R. E., and A. Henderson-Sellers (1988), Modeling tropical deforestation: A study of GCM land-surface parameterizations, *Q. J. R. Meteorol. Soc.*, **114**, 439–462, doi:10.1002/qj.49711448009.
- Dickinson, R. E., A. Henderson-Sellers, and P. J. Kennedy (1993), Biosphere-Atmosphere Transfer Scheme (BATS) version 1e as coupled to the NCAR Community Climate Model, *NCAR Tech. Note NCAR/TN-387+STR*, 72 pp., Natl. Cent. for Atmos. Res., Boulder, Colo.
- Dowhan, J., T. Halavik, A. Milliken, A. MacLachan, M. Caplis, K. Lima, and A. Zimba (1997), Calcareous habitats and Catskill High Peaks, in *Significant Habitats and Habitat Complexes of the New York Bight Watershed*, pp. 123–130, U.S. Fish and Wildlife Serv. South. N. Engl. – N. Y. Bight Coastal Ecosyst. Program, Charlestown, R. I.
- Eastman, J. L., M. B. Coughenour, and R. A. Pielke Sr. (2001), The regional effects of CO<sub>2</sub> and landscape change using a coupled plant and meteorological model, *Global Change Biol.*, **7**, 797–815, doi:10.1046/j.1354-1013.2001.00411.x.
- Epstein, C. M. (2003), Is the Pine Barrens water table declining? What does the record show?, in *Periglacial Features of Southern New Jersey: Field Guide and Proceedings of the Geological Association of New Jersey*, edited by M. J. Hozik and M. J. Mihalasky, pp. 51–78, Richard Stockton Coll. of N. J., Pomona.
- Fabian, M. S., and D. J. Burns (1966), The role of farmer-owned fruit and vegetable marketing organizations in New Jersey: part I: Present status, 57 pp., N. J. Agric. Exp. Stn., Dep. of Agric. Econ. and Marketing, Rutgers Univ., New Brunswick, N. J.
- Gallo, K. P., D. R. Easterling, and T. C. Peterson (1996), Notes and correspondence: The influence of land use/land cover on climatological values of the diurnal temperature range, *J. Clim.*, **9**, 2941–2944, doi:10.1175/1520-0442(1996)009<2941:TLOLUC>2.0.CO;2.
- Gedzelman, S. D., S. Austin, R. Cermak, N. Stefano, S. Partridge, S. Quisenberry, and D. A. Robinson (2003), Mesoscale aspects of the urban heat island around New York City, *Theor. Appl. Climatol.*, **75**, 29–42.
- Giorgi, F., and R. Avissar (1997), Representation of heterogeneity effects in earth system modeling: Experience from land surface modeling, *Rev. Geophys.*, **35**, 413–438, doi:10.1029/97RG01754.
- Grimmond, C. S. B., and T. R. Oke (1999), Heat storage in urban areas: Local-scale observations and evaluation of a simple model, *J. Appl. Meteorol.*, **38**, 922–940, doi:10.1175/1520-0450(1999)038<0922:HSIUAL>2.0.CO;2.
- Harrington, J. Y. (1997), The effects of radiative and microphysical processes on simulated warm and transition-season Arctic stratus, Ph.D. dissertation, 270 pp., Dep. of Atmos. Sci., Colo. State Univ., Fort Collins.

- Hart, J. F. (1991), The perimetropolitan bow wave, *Geogr. Rev.*, *81*, 35–51, doi:10.2307/215175.
- Heim, R. (1999), Climate of 1999: July drought in the U.S., *Clim. Serv. Div., Natl. Clim. Data Cent., Asheville, N. C.*, 13 Aug.
- Intergovernmental Panel on Climate Change (2007), *Climate Change 2007: The Physical Science Basis—Contribution of Working Group I to the Fourth Assessment Report of the Intergovernmental Panel on Climate Change*, edited by S. Solomon et al., Cambridge Univ. Press, New York.
- Jin, M., R. E. Dickinson, and D. L. Zhang (2005), The footprint of urban areas on global climate as characterized by MODIS, *J. Clim.*, *18*, 1551–1565, doi:10.1175/JCLI3334.1.
- Kain, J. S., and J. M. Fritsch (1992), The role of the convective trigger functions in numerical forecasts of mesoscale convective systems, *Meteorol. Atmos. Phys.*, *49*, 93–106, doi:10.1007/BF01025402.
- Kalnay, E., and M. Cai (2003), Impact of urbanization and land-use change on climate, *Nature*, *423*, 528–531, doi:10.1038/nature01675.
- Kalnay, E., et al. (1996), The NCEP/NCAR 40-year reanalysis project, *Bull. Am. Meteorol. Soc.*, *77*, 437–472, doi:10.1175/1520-0477(1996)077<0437:TNYRP>2.0.CO;2.
- Karl, T. R., H. F. Diaz, and G. Kukla (1988), Urbanization: Its detection and effect in the United States climate record, *J. Clim.*, *1*, 1099–1123, doi:10.1175/1520-0442(1988)001<1099:UIDAEI>2.0.CO;2.
- Karl, T. R., P. D. Jones, R. W. Knight, G. Kukla, N. Plummer, V. Razuvayev, K. P. Gallo, J. Lindsey, R. J. Charlson, and T. C. Peterson (1993), A new perspective on recent global warming: Asymmetric trends of daily maximum and minimum temperature, *Bull. Am. Meteorol. Soc.*, *74*, 1007–1023, doi:10.1175/1520-0477(1993)074<1007:ANPORG>2.0.CO;2.
- Klein Goldewijk, K. (2001), Estimating global land use change over the past 300 years: The HYDE database, *Global Biogeochem. Cycles*, *15*, 417–433, doi:10.1029/1999GB001232.
- Kuchler, A. W. (1964), The potential natural vegetation of the conterminous United States, *Spec. Publ. 36*, scale 1:3,168,000, Am. Geogr. Soc., New York.
- Lathrop, R., and J. Hasse (2006), Tracking New Jersey's changing landscape, in *New Jersey's Environments: Past, Present, and Future*, edited by N. M. Maher, pp. 111–127, Rutgers Univ. Press, New Brunswick, N. J.
- Letts, T. (1905), New maps, *Bull. Am. Geogr. Soc. N. Y.*, *37*, 497–502.
- Little, S. (1979), Fire and plant succession in the New Jersey Pine Barrens, in *Pine Barrens: Ecosystem and Landscape*, edited by R. T. T. Forman, pp. 297–314, Academic, New York.
- Little, S., and P. W. Garrett (1990), *Chamaecyparis thyoides* (L.) B.S.P.: Atlantic white-cedar, in *Silvics of North America*, vol. 1, *Conifers, Agric. Handbook*, vol. 654, pp. 103–108, U.S. For. Serv., U.S. Dep. of Agric., Washington, D. C.
- Lynn, B. H., D. Rind, and R. Avissar (1995), The importance of mesoscale circulations generated by subgrid-scale landscape heterogeneities in general circulation models, *J. Clim.*, *8*, 191–205, doi:10.1175/1520-0442(1995)008<0191:TIOMCG>2.0.CO;2.
- Mahmood, R., K. G. Hubbard, and C. Carlson (2004), Modification of growing-season temperature records in the Northern Great Plains due to land-use transformation: verification of modeling results and implication for global climate change, *Int. J. Climatol.*, *24*, 311–327, doi:10.1002/joc.992.
- Marshall, C. H., Jr., R. A. Pielke Sr., and L. T. Steyaert (2003), Crop freezes and land-use change in Florida, *Nature*, *426*, 29–30, doi:10.1038/426029a.
- Marshall, C. H., Jr., R. A. Pielke, L. T. Steyaert, and D. A. Willard (2004a), The impact of anthropogenic land-cover change on the Florida peninsula sea breezes and warm season sensible weather, *Mon. Weather Rev.*, *132*, 28–52, doi:10.1175/1520-0493(2004)132<0028:TIOALC>2.0.CO;2.
- Marshall, C. H., Jr., R. A. Pielke Sr., and L. T. Steyaert (2004b), Has the conversion of natural wetlands to agricultural land increased the incidence and severity of damaging freezes in South Florida?, *Mon. Weather Rev.*, *132*, 2243–2258, doi:10.1175/1520-0493(2004)132<2243:HTCONW>2.0.CO;2.
- Marshall, S. (2004), The Meadowslands before the commission: Three centuries of human use and alteration of the Newark and Hackensack Meadows, *Urban Habitats*, *2*, 4–27.
- Matthews, H. D., A. J. Weaver, M. Eby, and K. J. Meissner (2003), Radiative forcing of climate by historical land cover change, *Geophys. Res. Lett.*, *30*(2), 1055, doi:10.1029/2002GL016098.
- McCormick, J. (1979), The vegetation of the New Jersey Pine Barrens, in *Pine Barrens: Ecosystem and Landscape*, edited by R. T. T. Forman, pp. 229–243, Academic, New York.
- McCormick, J. and L. Jones (1973), The Pine Barrens: Vegetation geography, *Res. Rep. 3*, 76 pp., N. J. State Mus., Trenton.
- McQuilkin, W. E. (1935), Root development of pitch pine, with some comparative observations on shortleaf pine, *J. Agric. Res.*, *51*, 983–1016.
- Mellor, G. L., and T. Yamada (1982), Development of a turbulence closure model for geophysical fluid problems, *Rev. Geophys.*, *20*, 851–875, doi:10.1029/RG020i004p00851.
- Mölders, N. (2000), Similarity of microclimate as simulated in response to landscapes of the 1930s and the 1980s, *J. Hydrometeorol.*, *1*, 330–352, doi:10.1175/1525-7541(2000)001<0330:SOMASI>2.0.CO;2.
- Morehart, M., N. Gollehon, R. Dismukes, V. Breneman, and R. Heimlich (1999), Economic assessment of the 1999 drought: Agricultural impacts are severe locally, but limited nationally, *Agric. Inf. Bull.* 755, 20 pp., U.S. Dep. of Agric., Washington, D. C.
- Niyogi, D., T. Holt, S. Zhong, P. C. Pyle, and J. Basara (2006), Urban and land surface effects on the 30 July 2003 mesoscale convective system event observed in the southern Great Plains, *J. Geophys. Res.*, *111*, D19107, doi:10.1029/2005JD006746.
- National Research Council (2005), *Radiative Forcing of Climate Change: Expanding the Concept and Addressing Uncertainties*, edited by D. J. Jacob et al., 207 pp., Natl. Acad. Press, Washington, D. C.
- Offerle, B., C. S. B. Grimmond, and T. R. Oke (2003), Parameterization of net all-wave radiation for urban areas, *J. Appl. Meteorol.*, *42*, 1157–1173, doi:10.1175/1520-0450(2003)042<1157:PONARF>2.0.CO;2.
- Oke, T. R. (1982), The energetic basis of the urban heat island, *Q. J. R. Meteorol. Soc.*, *108*, 1–24.
- Oke, T. R. (1988), The urban energy balance, *Prog. Phys. Geogr.*, *12*, 471–508.
- Oleson, K. W., G. B. Bonan, S. Levis, and M. Vertenstein (2004), Effects of land use change on North American climate: Impact of surface datasets and model biogeophysics, *Clim. Dyn.*, *23*, 117–132, doi:10.1007/s00382-004-0426-9.
- Olsson, H. (1979), Vegetation of the New Jersey Pine Barrens: A phytosociological classification, in *Pine Barrens: Ecosystem and Landscape*, edited by R. T. T. Forman, pp. 245–263, Academic, New York.
- Pielke, R. A. (2001), Influence of the spatial distribution of vegetation and soils on the prediction of cumulus convective rainfall, *Rev. Geophys.*, *39*, 151–177, doi:10.1029/1999RG000072.
- Pielke, R. A., Sr. (2002), *Mesoscale Meteorological Modeling*, 2nd ed., 676 pp., Academic, San Diego, Calif.
- Pielke, R. A., and R. Avissar (1990), Influence of landscape structure on local and regional climate, *Landscape Ecol.*, *4*, 133–155, doi:10.1007/BF00132857.
- Pielke, R. A., G. Dalu, J. S. Snook, T. J. Lee, and T. G. F. Kittel (1991), Nonlinear influence of mesoscale land use on weather and climate, *J. Clim.*, *4*, 1053–1069, doi:10.1175/1520-0442(1991)004<1053:NIOMLU>2.0.CO;2.
- Pielke, R. A., R. Avissar, M. Raupach, A. J. Dolman, X. Zeng, and A. S. Denning (1998), Interactions between the atmosphere and terrestrial ecosystems: Influence on weather and climate, *Global Change Biol.*, *4*, 461–475, doi:10.1046/j.1365-2486.1998.t01-1-00176.x.
- Pielke, R. A., R. L. Walko, L. T. Steyaert, P. L. Vidale, G. E. Liston, W. A. Lyons, and T. N. Chase (1999), The influence of anthropogenic landscape changes on weather in south Florida, *Mon. Weather Rev.*, *127*, 1663–1673, doi:10.1175/1520-0493(1999)127<1663:TIOALC>2.0.CO;2.
- Pielke, R. A., Sr., et al. (2007), Unresolved issues with the assessment of multidecadal global land surface temperature trends, *J. Geophys. Res.*, *112*, D24S08, doi:10.1029/2006JD008229.
- Pitman, A. (2003), The evolution of, and revolution in, land surface schemes designed for climate models, *Int. J. Climatol.*, *23*, 479–510, doi:10.1002/joc.893.
- Ramankutty, N., and J. A. Foley (1999), Estimating historical changes in global land cover: Croplands from 1700 to 1992, *Global Biogeochem. Cycles*, *13*, 997–1027, doi:10.1029/1999GB900046.
- Rosenzweig, C., and W. D. Solecki (2001), Climate change and a global city: Learning from New York, *Environment*, *43*, 2–12.
- Rowe, P. B., and L. F. Reimann (1961), Water use by brush, grass, and grass-forb vegetation, *J. For.*, *59*, 175–181.
- Sailor, D. J. (1995), Simulated urban climate response to modifications in surface albedo and vegetative cover, *J. Appl. Meteorol.*, *34*, 1694–1704.
- Schmidt, H. G. (1973), *Agriculture in New Jersey: A Three-Hundred Year History*, 335 pp., Rutgers Univ. Press, New Brunswick, N. J.
- Schneider, N., W. Eugster, and B. Schichler (2004), The impact of historical land-use changes on the near-surface atmospheric conditions on the Swiss Plateau, *Earth Interact.*, *8*, 1–27, doi:10.1175/1087-3562(2004)008<0001:TIOHLC>2.0.CO;2.
- Schott, C. (1882), A comparison of the relative value of the polyconic projection used on the Coast and Geodetic Survey, with some other projections, in *Report of the Superintendent of the U.S. Coast and Geodetic Survey for the Fiscal Year Ending June 30, 1880*, pp. 287–296, U.S. Govt. Print. Off., Washington, D. C.
- Segal, M., and R. W. Arritt (1992), Non-classical mesoscale circulations caused by surface sensible heat-flux gradients, *Bull. Am. Meteorol. Soc.*,

- 73, 1593–1604, doi:10.1175/1520-0477(1992)073<1593:NMCCBS>2.0.CO;2.
- Sellers, P. J. (1992), Biophysical models of land surface processes, in *Climate System Modeling*, edited by K. E. Trenberth, pp. 451–490, Cambridge Univ. Press, New York.
- Sellers, P. J., et al. (1997), Modeling the exchanges of energy, water, and carbon between continents and the atmosphere, *Science*, *275*, 502–509, doi:10.1126/science.275.5299.502.
- Shepherd, J. M. (2005), A review of current investigations of urban-induced rainfall and recommendations for the future, *Earth Interact.*, *9*(12), 1–27.
- Shepherd, J. M., and S. J. Burian (2003), Detection of urban-induced rainfall anomalies in a major coastal city, *Earth Interact.*, *7*, 1–17, doi:10.1175/1087-3562(2003)007<0001:DOUIRA>2.0.CO;2.
- Shepherd, J. M., H. F. Pierce, and A. J. Negri (2002), Rainfall modification by major urban areas: Observations from spaceborne rain radar on the TRMM satellite, *J. Appl. Meteorol.*, *41*, 689–701, doi:10.1175/1520-0450(2002)041<0689:RMBMUA>2.0.CO;2.
- Shi, X., R. T. McNider, D. E. England, M. J. Friedman, W. LaPenta, and B. Norris (2005), On the behavior of the stable boundary layer and role of initial conditions, *Pure Appl. Geophys.*, *162*, 1811–1829, doi:10.1007/s00024-005-2694-7.
- Sidar, J. W. (1976), *George Hammell Cook: A Life in Agriculture and Geology*, 282 pp., Rutgers Univ. Press, New Brunswick, N. J.
- Stansfield, C. A. (1998), *A Geography of New Jersey: A City in the Garden*, 304 pp., Rutgers Univ. Press, New Brunswick, N. J.
- Steyaert, L. T., and R. A. Pielke (2002), Using Landsat-derived land cover, reconstructed vegetation, and atmospheric mesoscale modeling in environmental and global change research, paper presented at 53rd International Astronautical Congress, World Space Congress, Houston, Tex., 10–19 Oct.
- Sud, Y. C., J. Shukla, and Y. Mintz (1988), Influence of land surface-roughness on atmospheric circulation and precipitation: A sensitivity study with a general circulation model, *J. Appl. Meteorol.*, *27*, 1036–1054, doi:10.1175/1520-0450(1988)027<1036:IOLSRO>2.0.CO;2.
- Taha, H. (1997), Urban climates and heat islands: Albedo, evapotranspiration, and anthropogenic heat, *Energy Build.*, *25*, 99–103, doi:10.1016/S0378-7788(96)00999-1.
- Turner, B. L., II (2001), Land-use and land-cover change: Advances in 1.5 decades of sustained international research, *GALA Ecol. Perspect. Sci. Humanities Econ.*, *10*, 269–272.
- U.S. Bureau of the Census (1960), *Historical Statistics of the United States: Colonial Times to 1957, A Statistical Abstract Supplement*, 789 pp., Soc. Sci. Res. Council, U.S. Bur. of the Census, Washington, D. C.
- U.S. Department of Agriculture (1992), Land use and acres diverted: 1992 and 1987, *Census of Agriculture*, vol. 1, *New Jersey State Data*, 17 pp., U.S. Govt. Print. Off., Washington, D. C.
- U.S. Department of Agriculture (1999), *New Jersey Weekly Crop Progress Report*, vol. 60(10), National Agricultural Statistics Service, Washington, D. C., 7 June.
- Vermeule, C. C. (1889), Topographical atlas sheets 1–17, *Atlas of New Jersey, Geological Survey of New Jersey*, 62 × 88 cm, 1883–1889, Julius Bien and Co., New York.
- Vermeule, C. C. (1897), Drainage of the Hackensack and Newark tide-marshes, map of Hackensack Meadows, in *Geological Survey of New Jersey, Annual Report of the State Geologist for the Year 1896*, pp. 287–318, MacCrellish and Quigley, Trenton, N. J.
- Vogelmann, J. E., S. M. Howard, L. M. Yang, C. R. Larson, B. K. Wylie, and N. Van Driel (2001), Completion of the 1990s national land cover dataset for the conterminous United States from Landsat thematic mapper data and ancillary data sources, *Photogramm. Eng. Remote Sens.*, *67*, 650–662.
- Voegt, J. A., and T. R. Oke (1997), Complete urban surface temperatures, *J. Appl. Meteorol.*, *36*, 1117–1132, doi:10.1175/1520-0450(1997)036<1117:CUST>2.0.CO;2.
- Waisanen, P. J., and N. B. Bliss (2002), Changes in population and agriculture land in conterminous United States counties, 1790 to 1997, *Global Biogeochem. Cycles*, *16*(4), 1137, doi:10.1029/2001GB001843.
- Walko, R. L., and C. J. Trempack (2000), Regional Atmospheric Modeling System Users Guide: Version 4.2MRC, ASTeR internal report, ASTeR Div., Mission Res. Corp., Fort Collins, Colo.
- Walko, R. L., W. R. Cotton, J. L. Harrington, and M. P. Meyers (1995), New RAMS cloud microphysics parameterization. Part I: The single-moment scheme, *Atmos. Res.*, *38*, 29–62, doi:10.1016/0169-8095(94)00087-T.
- Walko, R. L., et al. (2000), Coupled atmosphere-biophysics-hydrology models for environmental modeling, *J. Appl. Meteorol.*, *39*, 931–944, doi:10.1175/1520-0450(2000)039<0931:CABHMF>2.0.CO;2.
- Weaver, C. P. (2004a), Coupling between large-scale atmospheric processes and mesoscale land-atmosphere interactions in the U.S. Southern Great Plains during summer: Part I. Mesoscale case studies, *J. Hydrometeorol.*, *5*, 1223–1246, doi:10.1175/JHM-396.1.
- Weaver, C. P. (2004b), Coupling between large-scale atmospheric processes and mesoscale land-atmosphere interactions in the U.S. Southern Great Plains during summer: Part II. Large-scale-mean impacts of the mesoscale, *J. Hydrometeorol.*, *5*, 1247–1258, doi:10.1175/JHM-397.1.
- Weaver, C. P., and R. Avissar (2001), Atmospheric disturbances caused by human modification of the landscape, *Bull. Am. Meteorol. Soc.*, *82*, 269–281, doi:10.1175/1520-0477(2001)082<0269:ADCBHM>2.3.CO;2.
- Wichansky, P. S., C. P. Weaver, L. T. Steyaert, and R. L. Walko (2006), Evaluating the effects of historical land cover change on summertime weather and climate in New Jersey, in *New Jersey's Environments: Past, Present, and Future*, edited by N. M. Maher, pp. 128–163, Rutgers Univ. Press, New Brunswick, N. J.
- Widmann, R. H. (2002), Trends in New Jersey forests, *Pap. NE-INF-148-02*, Northeast Res. Stn., For. Serv., U.S. Dep. of Agric., Newtown Square, Pa.
- Xiao, Q., E. G. McPherson, J. R. Simpson, and S. L. Ustin (1998), Rainfall interception by Sacramento's urban forest, *J. Arboriculture*, *24*, 235–244.
- Yoshikado, H. (1990), Vertical structure of the sea breeze penetrating through a large urban complex, *J. Appl. Meteorol.*, *29*, 878–891, doi:10.1175/1520-0450(1990)029<0878:VSOTSB>2.0.CO;2.
- Yoshikado, H. (1992), Numerical study of the daytime urban effect and its interaction with the sea breeze, *J. Appl. Meteorol.*, *31*, 1146–1164, doi:10.1175/1520-0450(1992)031<1146:NSOTDU>2.0.CO;2.
- Zeng, X., R. E. Dickinson, A. Walker, M. Shaikh, R. S. DeFries, and J. Qi (2000), Derivation and evaluation of global 1-km fractional vegetation cover data for land modeling, *J. Appl. Meteorol.*, *39*, 826–839, doi:10.1175/1520-0450(2000)039<0826:DAEOGK>2.0.CO;2.
- Zhao, M., A. J. Pitman, and T. N. Chase (2001), The impact of land cover change on the atmospheric circulation, *Clim. Dyn.*, *17*, 467–477, doi:10.1007/PL00013740.

L. T. Steyaert, Center for Earth Resources Observation and Science, U.S. Geological Survey, Biospheric Sciences Branch, NASA Goddard Space Flight Center, Greenbelt, MD 20771, USA.

R. L. Walko, Department of Civil and Environmental Engineering, Duke University, Durham, NC 27708, USA.

C. P. Weaver and P. S. Wichansky, Center for Environmental Prediction and Department for Environmental Sciences, Rutgers University, New Brunswick, NJ 08901, USA. (pstuart@cep.rutgers.edu)